AN ABSTRACT OF THE THESIS OF

Reina Nakamura for the degree of Master of Science in Atmospheric Sciences presented on October 21, 1999. Title: Local and Area-Averaged Momentum Fluxes.

Abstract Approved: Redacted for privacy

Larry Mahrt

Aircraft and tower data are analyzed to 1) estimate the area-averaged and local momentum roughness lengths over various surfaces 2) examine the applicability of the ψ-stability formulations of Paulson (1970) and Dyer (1974) for unstable and stable conditions respectively for predicting momentum fluxes and 3) investigate the possibility that BOREAS tower flux measurements were made in the roughness sublayer. For these purposes, BOREAS 94 and Microfronts tower data as well as aircraft data from BOREAS 94, BOREAS 96 and SGP aircraft data are analyzed. In stable conditions, the Dyer ψ-stability formulation predicts the tower-based local momentum fluxes reasonably well both over the forest and grassland. In unstable conditions, however, the Paulson ψ-stability formulation tends to overpredict the local momentum flux measured by towers over forest canopies. The same formulation estimates the aircraft-based area-averaged momentum fluxes over forests well despite some weak heterogeneity of the surface. The Paulson-ψ stability formulation also correctly predicts the local momentum flux based on towers over grassland. Thus, tower

measurements over forest canopies in unstable conditions incorporate systematic bias, which may be associated with the possibility that the tower measurements were not above the roughness sublayer. This hypothesis is investigated in some detail.

Local and Area-Averaged Momentum Fluxes

by

Reina Nakamura

A Thesis Submitted

to

Oregon State University

In partial fulfillment of
the requirements for the
degree of

Master of Science

Presented October 21, 1999
Commencement June 2000

Master of Science thesis of Reina Nakamura presented on October 21,1999

Approved:

Redacted for privacy

Major Professor, representing Atmospheric Sciences

Redacted for privacy

Dean of College of Oceanic and Atmospheric Sciences

Redacted for privacy

Dean of Graduate School

I understand that my thesis will become part of the permanent collection of Oregon State University libraries. My signature below authorizes release of my thesis to any reader upon request.

Redacted for privacy

Reina Nakamura, Author

ACKNOWLEDGMENTS

I would like to thank everyone who has given me support and encouragement without which I could not have finished this piece of work.

The tremendous knowledge, support and encouragement of my advisor Dr. Larry Mahrt have allowed me to complete this work. I have been frequently helped by his calmness and humor to cool down and move forward in the rough times of my research.

The Boundary Layer Group members, in particular, Dean Vickers and John Wong have helped me out with programming and technical problems.

My friend/colleague Mark Matheson has patiently provided me with a magnificent amount of encouragement and support in the long process of my thesis work. He has also been the most excellent sounding board of all ever. Thanks!

The presence of my friends/colleagues Scott Bennett and Nicolai Thum has been of great support both in science and daily life. Gracias and Danke!

My friend Maho Wichert-Takeda has frequently saved me from hard times and given me hope. Domo arigato!

The warm encouragement and enthusiasm in science of my mentor, Haydee Salmun at the Johns Hopkins University cannot forget to be acknowledged. Despite the physical distance, she has always been present in my path.

Support for this work was provided by National Science Foundation 9807768-ATM.

TABLE OF CONTENTS

TABLE OF CONTENTS (CONTINUED)

LIST OF FIGURES

LIST OF FIGURES (CONTINUED)

Figure Page

LIST OF FIGURES (CONTINUED)

Figure Page

LIST OF TABLES

LIST OF APPENDIX FIGURES

LIST OF APPENDIX TABLES

Table Page

Local and Area-Averaged Momentum Fluxes

1. Introduction

Monin-Obukhov (M-O) similarity theory and its accompanying stability functions were formulated empirically to describe fluxes of momentum and other quantities in the turbulent surface layer over a strictly homogeneous surface with stationary flow. For these conditions, the theory works well. In contrast to the premises of M-O similarity theory, the actual earth's surface is generally heterogeneous. No formal theory to describe turbulence flux-gradient relationship over a heterogeneous surface has been established. Therefore, we must rely on and start with M-O similarity theory to characterize the momentum properties in the turbulent surface layer over the earth's heterogeneous surface.

In M-O similarity theory, the momentum roughness length represents the mechanical influence of the surface on the flux-gradient relationship in the surface layer. The magnitude of the roughness length is related to the dimensions of the actual roughness elements of the surface, but assumed to be independent of the atmospheric stability. The ψ-stability function describes the influence of stability in the surface layer on the turbulence and the flux-gradient relationship. In numerical models, the momentum flux at the surface of an area represented by a grid point is computed from a bulk aerodynamic formula using values of the wind

speed, temperature and humidity. This formula requires specification of the momentum roughness length and ψ-stability function.

The present study has three objectives: 1) estimate the magnitudes of the momentum roughness lengths based on local fluxes and area-averaged fluxes for various surface types, using data from neutral surface layers, 2) examine whether M-O similarity theory and its accompanying ψ-stability functions can be used to formulate fluxes over forest canopies and area-averaged fluxes over various surface types and 3) investigate if the towers in the BOREAS experiment were situated in the roughness sublayer. Numerous micrometeorological data sets acquired by aircraft and towers over forest canopies and agricultural fields are analyzed, as described in Sections 3 and 4. We first review aspects of M-O similarity theory relevant to this study.

2. Background

2.1 Monin-Obukhov Similarity Theory

Based on similarity scaling, Monin and Obukhov (1954) proposed a similarity theory to describe a stationary turbulent wind field in the surface layer over a homogeneous surface. In the neutral surface layer, the gradient of the mean wind speed, U, with respect to height, z, can be expressed as

$$\frac{\partial U}{\partial z} = \frac{u*}{z\kappa} \tag{1}$$

where $u*$ is the friction velocity defined as

$$u* \equiv \sqrt[4]{\overline{u'w'}_s^{\,2} + \overline{v'w'}_s^{\,2}} = \sqrt{\frac{\tau_s}{\rho}}$$

where "s" indicates values at the surface. The parameter κ is the von Karman constant often taken to be 0.4 as is done in this study.

If we divide both sides of equation (1) by $u*/z\kappa$, we obtain the dimensionless wind shear of the surface layer, equal to unity for neutral conditions,

$$\phi = \frac{\kappa z}{u*}\frac{\partial u}{\partial z} = 1 \qquad (2)$$

The effect of stability (buoyancy fluxes) can be expressed in terms of z/L, often written as ζ, where z is the height above the ground and L is the Obukhov length defined as

$$L \equiv -\frac{\overline{\theta_v} u*^3}{\kappa g \left(\overline{w'\theta_v'}\right)_s}$$

where g is the acceleration due to gravity, θ_v the virtual potential temperature and $w'\theta_v'_s$ the kinematic virtual heat flux at the surface. Thus, the dimensionless shear becomes a function of ζ

$$\phi(\zeta) = \frac{\kappa\zeta}{u*}\frac{\partial u}{\partial \zeta} = \frac{\kappa\left(\frac{z}{L}\right)}{u*}\frac{\partial u}{\partial\left(\frac{z}{L}\right)} = \frac{\kappa z}{u*}\frac{\partial u}{\partial z} \qquad (3)$$

By definition, the extrapolated mean wind speed diminishes to zero at the height z_{om}, the momentum roughness length. We can integrate equation (2) from z_{om} to z to obtain a bulk aerodynamic relationship of the surface layer between the two heights,

$$U = \frac{u^*}{\kappa}\left[\ln\left(\frac{z}{z_{om}}\right) - \psi(\zeta)\right] \tag{4}$$

where U is the wind speed at height z and ψ is defined as

$$\psi \equiv \int_{\frac{z_{om}}{L}}^{\zeta} \frac{1-\phi(\xi')}{\xi'} d\xi' \tag{5}$$

where ξ' is a dummy variable of integration. The stability correction ψ vanishes at neutral conditions ($\zeta = 0$). The actual formulation of ψ as a function of ζ has to be determined empirically either directly or by integration of ϕ. Note if the displacement height d_o needs to be introduced, the height z in equations (1) to (5) becomes (z - d_o).

M-O similarity theory requires that the turbulent wind field be stationary and over a homogeneous surface. M-O similarity is valid only at heights both considerably higher than the momentum roughness length, z_{om}, and significantly lower than the height of the boundary layer, Z_i.

2.2 Area-Averaged Momentum Roughness Length

Computing the area-averaged momentum roughness length is complicated, and the methodology is a source of controversy. Since the earth's surface is

generally heterogeneous, even a region corresponding to a small grid cell in a numerical model will likely be heterogeneous. Computing roughness lengths of heterogeneous surfaces is not an exceptional case, but a frequent necessity. The roughness length intended to represent the momentum flux over a heterogeneous surface is called an effective roughness length, often denoted as z_{om}^{eff}. In the past, a number of methodologies were proposed to compute this parameter. These methodologies can be grossly classified into two approaches.

The goal of the first approach is to estimate the correct spatial-averaged surface layer wind speed (e.g. Taylor, 1987). The second approach has been formulated to estimate the correct spatial-averaged surface stress (e.g. Claussen, 1990; Mason, 1998, Goode and Belcher, manuscript). The second approach may be preferable for application to GCMs and weather forecast models since it gives the correct parameterization of the dynamical effect of the boundary layer on the large-scale synoptic motions (Goode and Belcher, manuscript).

The properties of the effective momentum roughness length according to these approaches have been investigated with atmospheric flows over heterogeneous surfaces simulated by numerical models. These investigations included sensitivity tests of the magnitudes and arrangements of local roughness lengths to the effective momentum roughness length and to the area-averaged flux. In all of these simulations, the surface types varied periodically and had distinct borders between individual homogeneous surfaces, for which the local momentum

roughness length could be specified (e.g. Taylor, 1987; Mason, 1988; Claussen, 1990; Goode and Belcher, manuscript).

The exact position of borders between homogeneous surfaces and the scale of heterogeneity need to be precisely defined in these approaches for computing the effective momentum roughness length. However, this premise may be far from reality in geophysical situations, where various scales of surface heterogeneity are superimposed.

Mahrt and Ek (1993) realized this problem, and used unweighted area-averaged momentum fluxes observed by aircraft, along with M-O similarity theory and existing ψ-stability functions to calculate a z_{om}^{eff} of a mixed agricultural region. However, their aircraft data were taken at approximately 100 m above the ground, which may have been above the surface layer. The present study takes a similar approach to Mahrt and Ek (1993), but analyzes aircraft data collected approximately 30 m above the vegetation canopy.

2.3. The ψ-Stability Function

Previous observational analyses are more often posed in terms of the ϕ-stability function than the ψ-stability function. The direct estimate of the value of ψ is more vulnerable to random errors compared to the calculation of ϕ (Sun, manuscript). However, computation of the value of ϕ requires very accurate

measurements of the vertical gradient of the mean wind speed and measurements at multiple levels above the roughness sublayer.

In order to obtain the value of ψ, one may integrate ϕ with respect to z or solve equation (4) for ψ directly, which requires only one measurement level above the roughness sublayer and does not require estimates of the wind shear.

If equation (4) is rearranged as

$$u^* = \frac{\kappa U}{\ln\left(\frac{z}{z_{om}}\right) - \psi(\zeta)} \tag{6}$$

the implication of the ψ-stability function becomes clearer. The larger the value of ψ, the more vigorous the turbulent mixing as indicated by a larger value of the friction velocity for a given wind speed. The value of ψ becomes positive in unstable conditions, associated with enhanced turbulent mixing. Similarly, the value of ψ becomes negative in stable conditions associated with suppression of turbulent mixing by stratification.

The present study evaluates the ψ-stability function formulated by Paulson (1970) for unstable conditions and the ψ-stability function from the integration of the ϕ-stability function formulated by Dyer (1974) for stable conditions. The lower limit of integration in (5) was taken to be zero in Paulson (1970) and Panofsky (1963) since roughness lengths are usually much smaller than L. For unstable conditions, the ψ-function becomes (Paulson, 1970)

$$\psi = 2\ln\left[\frac{1+x}{2}\right] + \ln\left[\frac{1+x^2}{2}\right] - 2\tan^{-1} x + \frac{\pi}{2}$$

with

$$x = (1-16\zeta)^{\frac{1}{4}}$$

and for stable conditions (Dyer, 1974)

$$\psi = -5\zeta$$

3. Data

3.1 Tower Data

Tower data sets from two field campaigns, the Boreal Ecosystem Atmosphere Study (BOREAS) 94 (boreal forests) and Microfronts 95 (grassland), are analyzed.

The boreal forest data were collected in central Canada in 1994 (Sellers et al., 1997). A total of 5 BOREAS study sites included towers with flux measurements applicable to the current analysis: Old Aspen North (OA), Old Black Spruce North (OBSN), Old Black Spruce South (OBSS), Old Jack Pine South (OJPS) and Young Jack Pine South (YJPS). (The wind speed and flux measurements were made at 10 m and 9.1 m respectively on the YJPS tower, therefore, the wind speed is interpolated to the 9.1m level.) The flux measurements above the canopy height adequate for the present study, were made at only one level above the canopy at all of the sites except the OA site, which included two levels above the canopy. An averaging window of 30 minutes was applied to the fluxes at all the BOREAS study sites.

Microfronts 95 took place in rangeland near De Graf, Kansas, about 35 miles northeast of Witchita. This site was characterized by a gently rolling surface with no major obstacles within several kilometers of the tower. The raw data were collected at 3 m- and 10 m-heights on a tower at the rate of 10 Hz. The processed

data set includes the momentum and heat fluxes, which were computed with a filtering window of 10 minutes and an averaging window of one hour.

3.2 Aircraft Data

Aircraft data sets from BOREAS 94, BOREAS 96 and Southern Great Plains Experiment (SGP) are analyzed. The BOREAS aircraft data sets were acquired by the Canadian Twin Otter aircraft (aircraft speed 55 m/s) over several study sites at an average altitude of 30 – 35 m. The same flight track was repeated sequentially by usually six or more passes to reduce random flux errors. The fluxes were sampled at a rate of 16 Hz. The wind, temperature and moisture data were filtered with a filtering window of 4km, to compute pass-averaged fluxes.

Twin Otter data from 7 BOREAS study sites are available for the analysis: OA, OBSN, OBSS, Grid DE, Grid FG, Old Jack Pine North (OJPN) and Young Jack Pine North (YJPN). Grid DE and Grid FG are mainly covered by spruce trees.

In the SGP experiment, the Twin Otter and Long EZ aircraft collected data at 32 Hz with a ground speed of 57 m/s and at 50 Hz with a ground speed of 55 m/s, respectively. The aircraft flew at an average altitude of 35 m over the track. The analyzed data was sampled over the El Reno track, which was 12-14 km in length. The El Reno track is covered mainly by grass, winter wheat and bare fields, and is located west of Oklahoma City. Turbulent fluxes were calculated with a 1-km filtering window. The aligned variable fields, including all fluxes, were

averaged with a 1-km running-mean window. The 1-km window was sequentially moved 250 m at a time.

4. Calculation Methods

4.1 Local Momentum Roughness Length

The tower data sets contain continuous measurements of the turbulence flux for the entire diurnal period. The data acquired between 1100 and 1500 local are taken to be the daytime data and those acquired between 2100 and 0500 local to be the nighttime data. We eliminate data taken during the nonstationary transition periods, when M-O similarity theory is not strictly applicable. In the present study, no further consideration of the stationarity of the wind field is applied as a data selection criterion. Some scatter in the results may be expected due to data points from non-stationary boundary layers occurring outside the transition periods.

The momentum roughness length is determined by the surface footprint over which eddies have traveled. Therefore, with surface heterogeneity the momentum roughness length becomes a function of wind direction. In order to compute the momentum roughness length as a function of the wind direction, data from tower sites in BOREAS are divided into 8 sectors according to the wind directions: 0°-45°, 45°-90°, 90°-135°, 135°-180°, 180°-225°, 225°-270°, 270°-315° and 315°-360°. For Microfronts data, the momentum roughness length is determined without partitioning the data according to the wind direction because of the fewer number of data points and the relatively homogeneous surface.

The local flux and other variables measured at one-level (for each of the 8 wind-directions in BOREAS) for each study site is applied to equation (4) to compute the local momentum roughness length. (Details of how to obtain variables in equation (4) are given in appendix 1.) This is called the flux method. Another method, the profile method, involves applying a linear least-square regression to the wind profile measured at multiple levels in neutral conditions. Sun (manuscript) compared these methods and found that the flux method, which uses fluxes measured only at one-level, is more vulnerable to random variations in the wind and stress fields than the profile method. On the other hand, the profile method requires evaluations of ϕ, which has its own difficulties as explained earlier in Section 2.3. Since most towers had local flux measurements only at one level, the flux method rather than the profile method is applied in order to include more study sites in the current analysis.

For each of the BOREAS study sites, the displacement height of the canopy is set to 2/3 of the average tree heights at each study site, an approximation commonly used for types of vegetation similar to those in BOREAS. (The sensitivity test of the results to changes in d_o is given in appendix 4.) The average tree height of an individual study site is determined by averaging the tree height of all species in proportion to the abundance of the species. The average heights and abundance of species at each BOREAS study site are reported in Sellers et al. (1994).

Since the sampling errors often become large for weak wind speeds and fluxes, the data collected under these conditions should be discarded in determining the momentum roughness length. Records with wind speed less than 2 m/s and friction velocity smaller than 0.5 m/s are not used for the calculation of the roughness length. The computed momentum roughness length for each wind direction over various study sites with these conditions is plotted against the stability as in Figure 1. Note that these roughness lengths are computed with the temporary assumption that the ψ-stability function by Paulson (1970) (Paulson ψ-function or formulation) can predict the value of ψ accurately, given the stability z/L computed from flight averaged fluxes. Since the parameter ψ has the least effect in near-neutral conditions ($\psi \approx 0$), values of the area-averaged momentum roughness lengths computed from flights in the near neutral surface layer can be taken for the final area-averaged momentum roughness length. A simple average of all the momentum roughness lengths falling into the near neutral category is taken as the local momentum roughness length of a study site. Since the roughness length appears inside a logarithm in equation (4), we are mainly interested in its order of magnitude. The exact definition of the near-neutral conditions varies between flights in order to have enough data points for averaging, but is typically $-0.1 < \zeta < 0.1$.

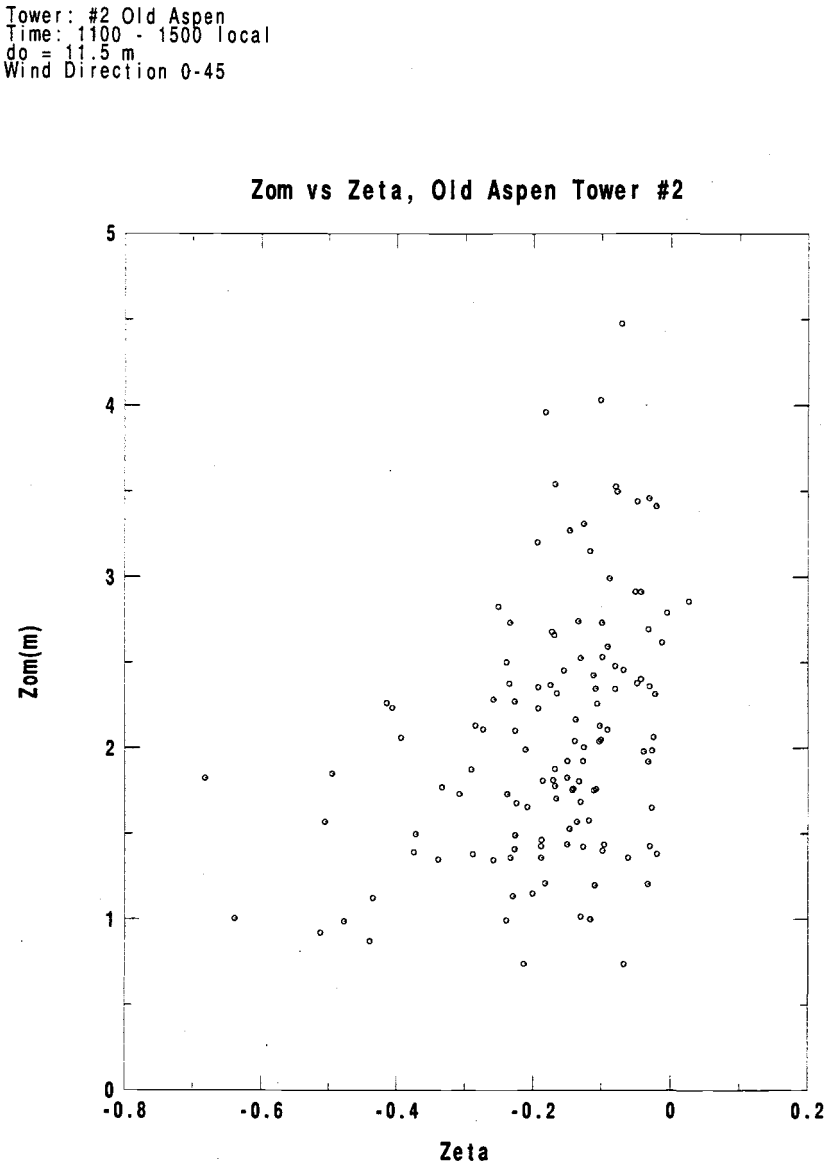

Figure 1. Momentum roughness lengths using Paulson–ψ formulation versus stability, ζ. BOREAS Old Aspen tower site, wind directions between 0 and 45°.

4.2 Area-Averaged Momentum Roughness Length

The aircraft were able to collect data only in the daytime, mainly in near-neutral or unstable conditions. In almost all cases, the data between 1000 and 1600 local are analyzed to avoid transition periods.

The area-averaged roughness length is computed in two ways. In the first method, the relevant variables appearing in equation (4) are flight-averaged over all of the passes, which are then directly used to compute the flight-averaged momentum roughness length. In the second method, the variables are pass-averaged to compute the pass-averaged momentum roughness lengths, which are then averaged over the flight. In both methods, the vector components rather than the magnitude of the vectors are averaged to be consistent with models, which use vector-averaged wind speeds and stresses.

Mahrt and Ek (1993) point out that the first method can be physically ambiguous since the averaging may incorporate nonstationarity before computing the ratios. However, this method is more mathematically sound in that it avoids the statistical problem of averaging ratios. In contrast to the first method, the second method is physically more meaningful, but statistically problematic due to the averaging of ratios.

The area-averaged roughness lengths computed with the two proposed methods differ from one another by an average of only 12%. The first method is selected to compute the area-averaged roughness length for this study. In stationary

cases, random flux errors are larger for pass-averaged variables than for flight-averaged variables. In non-stationary cases, errors due to nonstationarity are larger for flight-averaged variables. Since random flux errors are more problematic than errors due to nonstationarity, the flight-averaged fluxes are applied.

Note that this computation method of area-averaged momentum roughness length is slightly different from Mahrt and Ek (1993). In the present study, the area-averaged momentum roughness length is determined from area-averaged fluxes of near-neutral conditions only. This procedure becomes relevant if the formulated ψ-stability function is found to be inapplicable over heterogeneous surfaces. In that case, the area-averaged momentum roughness length determined from the entire range of stability as in Mahrt and Ek (1993) becomes questionable since the momentum roughness length is directly influenced by errors in the value of ψ.

4.3 Additional Area-Averaged Momentum Roughness Length for SGP Study Site

As described in Section 3.2., the SGP data available for the present study contains a series of turbulent fluxes for 1-km-running-mean windows over the El Reno flight track. This data enables us to compute the spatial variation of the momentum roughness length over the flight track in the same way as in Mahrt and Ek (1993). The area-averaged momentum roughness length is computed for each

of the 1km running-mean windows by presuming the applicability of the Paulson ψ-formulation since the window-averaged stability is not necessarily near-neutral. The logarithm of the values of the momentum roughness lengths for the 1-km-windows are averaged according to Taylor (1987) to obtain an area-averaged momentum roughness length along the entire flight track for each flight. The same spatial series of roughness lengths is also directly averaged over the flight track for comparison.

5. Results for Tower Data Analyses

5.1 Local Momentum Roughness Length

The computed local momentum roughness lengths of the BOREAS and Microfronts tower sites are summarized in Table 1. The BOREAS YJPS tower had two sonic anemometers (ATI-made and CAM-made), thus two sets of momentum roughness lengths of 8 sectors for the tower site were computed. The momentum roughness length of each site is computed from daytime and nighttime near-neutral conditions separately to confirm that the momentum roughness length is independent of thermal conditions and time of day. Table 1 shows a dependence of the momentum roughness length on wind direction.

5.2 Applicability of Paulson- and Dyer-ψ Stability Formulations

Given a local momentum roughness length determined for each study site from near-neutral conditions, the quantity ψ becomes the only unknown variable in equation (4). Thus, the value ψ can be solved from equation (4) and plotted against the stability along with the values of ψ predicted by Paulson (1970) and Dyer (1974) ψ-formulations.

The Paulson and Dyer ψ-formulations are strictly based on the best fit to experimental data acquired over relatively homogeneous terrain. Dyer and Hicks

Table 1. The momentum roughness lengths (m) for the BOREAS and Microfronts tower sites determined from near-neutral conditions for 8 wind direction groups. The daytime and nighttime data are analyzed separately to compute the momentum roughness lengths. ND stands for not determined.

Study Sites	OA, Tower #2 z = 39.5 m, d_o = 11.5 m		OBSN, Tower #3 z = 29m, d_o = 5.5 m		YJPS, Tower #4 (ATI) z = 9.1 m, d_o = 3 m		YJPS, Tower #4 (CAM) z = 9.1 m, d_o = 3 m	
Wind Directions	Daytime	Nighttime	Daytime	Daytime	Nighttime	Nighttime	Daytime	Nighttime
0 – 45 °	2.4	2.1	0.78	0.75	ND	ND	0.58	ND
45 – 90 °	2.0	2.1	1.0	1.1	0.45	ND	0.41	ND
90 – 135 °	2.3	2.5	1.6	1.8	0.53	ND	0.55	ND
135 – 180 °	1.7	1.8	1.3	1.2	0.60	ND	0.58	ND
180 – 225 °	2.4	2.1	1.1	0.92	0.68	ND	1.0	ND
225 – 270 °	2.6	2.6	1.6	1.7	0.57	0.63	1.1	0.62
270 – 315 °	2.0	1.7	1.6	1.6	0.53	0.81	0.68	0.80
315 – 360 °	2.6	2.4	1.3	1.3	0.52	ND	0.53	ND

Study Sites	OJPS, Tower #5 z = 20.0 m, d_o = 8.9 m		OBSS, Tower # 7 z = 26 m, d_o = 7.2 m		Microfronts z =10 m, d_o = 0 m		z =3 m, d_o = 0 m	
Wind Directions	Daytime	Nighttime	Daytime	Nighttime	Day	Night	Day	Night
0 – 45 °	1.7	1.8	0.9	1.2				
45 – 90 °	1.2	1.4	ND	ND				
90 – 135 °	1.3	1.6	1.1	ND				
135 – 180 °	1.3	1.3	1.1	ND	0.016	0.015	0.016	0.019
180 – 225 °	1.5	ND	0.93	ND				
225 – 270 °	1.5	1.3	0.88	1.2				
270 – 315 °	1.3	1.6	0.96	1.2				
315 – 360 °	1.5	1.5	0.92	0.94				

(1970) and Dyer (1974) imply that the ψ formulation by Paulson (1970) is valid only for the stability range of $-1 < \zeta < 0$. Later, data in Högström, (1988) supported the formulation to be valid for at least up to $-2 < \zeta < 0$. (Högström (1988) made a modification to Dyer (1974) which has negligible consequence for this analysis.) The experimental data of Högström (1988) indicates that the ψ formulation by Dyer (1974) for stable conditions is applicable for $0 < \zeta < 0.5$.

Despite the limited stability range of the applicability of the Paulson and Dyer ψ-formulations, numerical modelers rely on these formulations for all stabilities. Therefore, the applicability of the Paulson and Dyer ψ-formulations for predicting the momentum fluxes will be investigated over a larger range than just $-2 < \zeta < 0.5$.

Figures 2 - 9 show computed and predicted values of ψ plotted against the stability for the 8 wind directions at the OA site. Figures 10 - 15 show similar calculations for all the wind directions combined at each BOREAS study site. Figure 16 shows bin-averaged computed values of ψ versus the stability from all the BOREAS study sites. Bin-widths are chosen to provide enough data for statistically meaningful averaging. Consequently, the bin-widths vary from one data set to another.

In the stable case, the values of ψ computed from local flux measurements from the BOREAS towers agree with the Dyer ψ-formulation well, especially for $\zeta < 0.5$, in that a significant bias is not observed. For $\zeta > 0.5$, the computed and

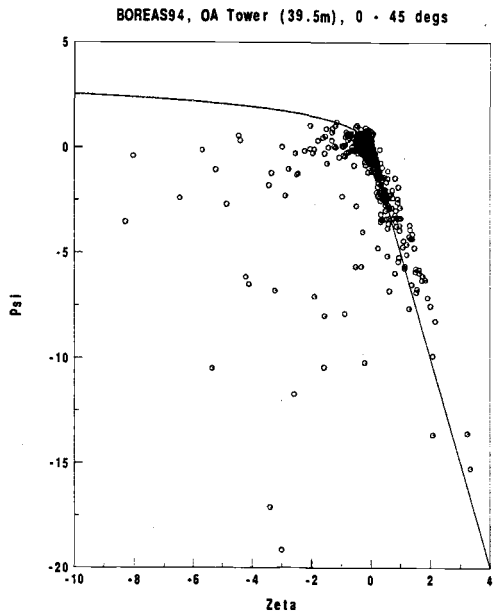

2a

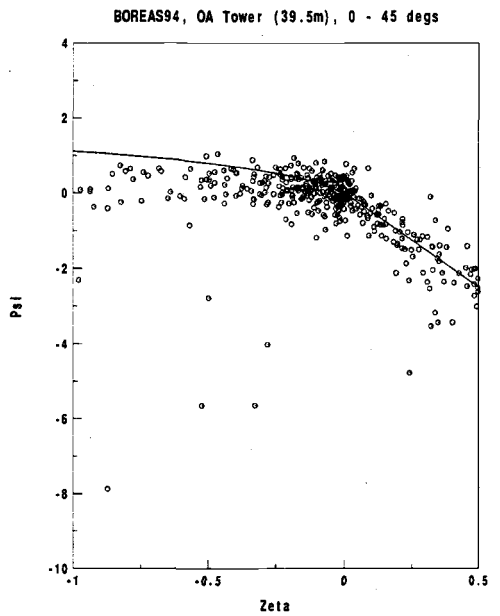

2b

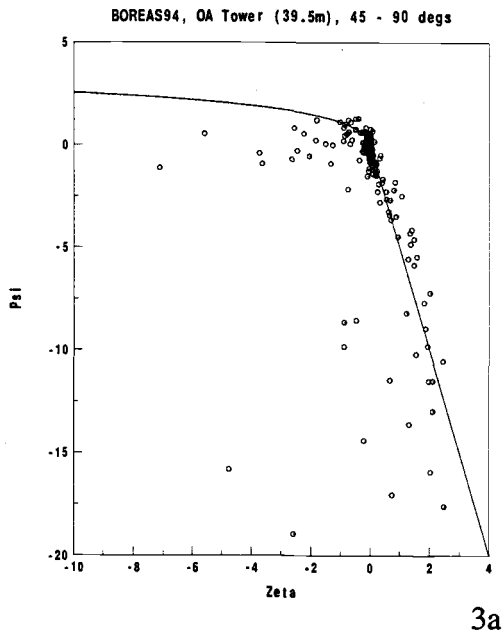

3a

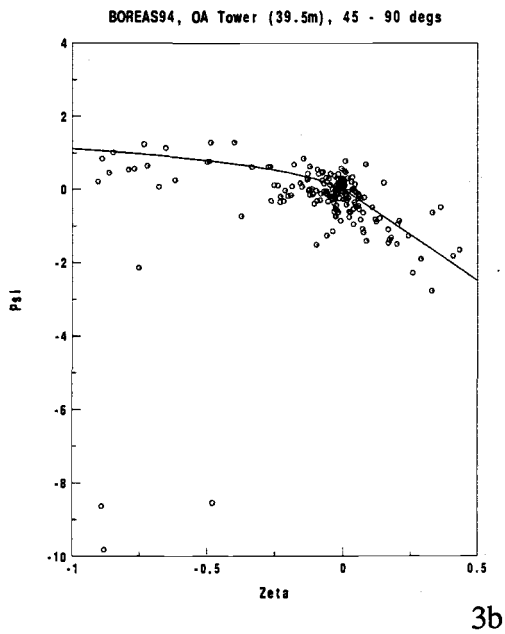

3b

Figure 2. Computed and predicted values of ψ (dots and line, respectively) plotted against the stability parameter ζ for wind directions 0-45° at BOREAS OA site. 2b is an enlargement of 2a to show more detail. Predicted values are based on Paulson (1970) and Dyer (1974).

Figure 3. Same as Figure 2 except for wind directions 45-90°.

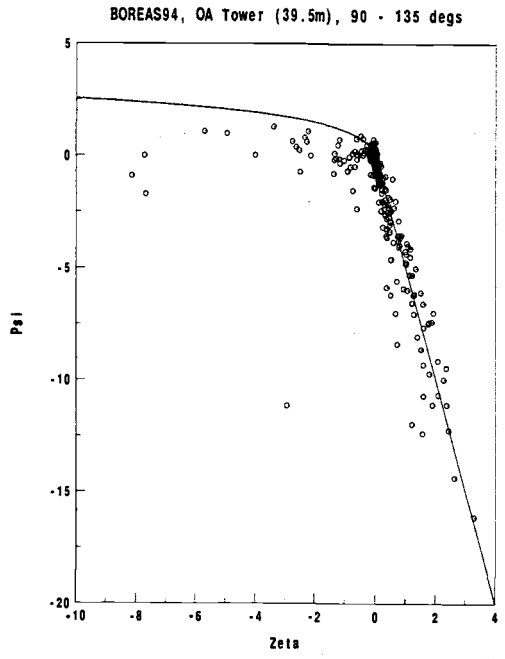

4a

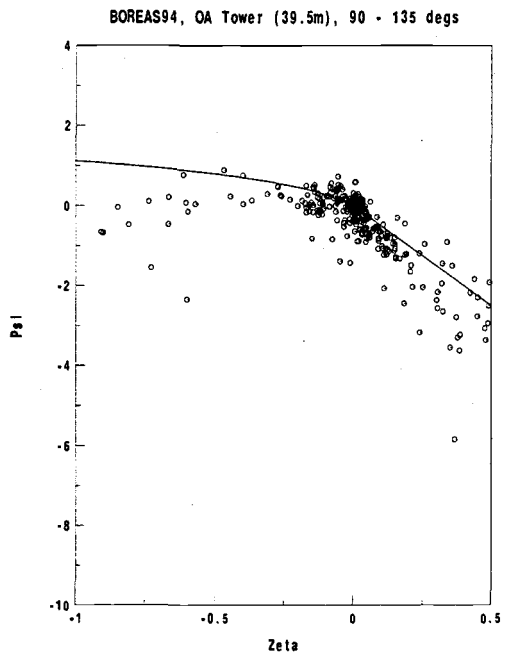

4b

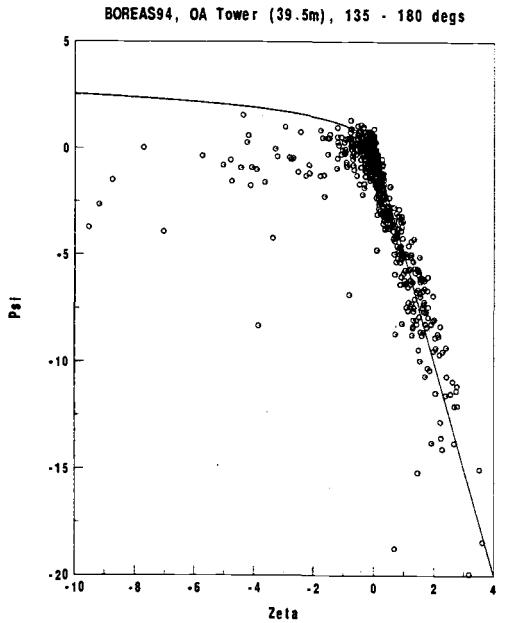

5a

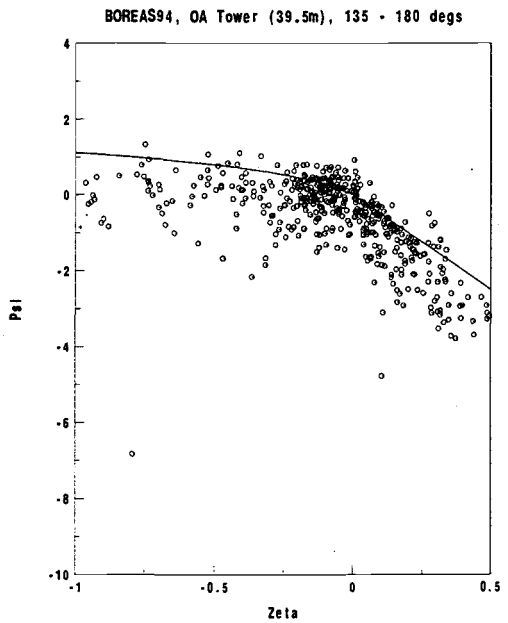

5b

Figure 4. Same as Figure 2 except for wind directions 90 - 135°.

Figure 5. Same as Figure 2 except for wind directions 135 - 180°.

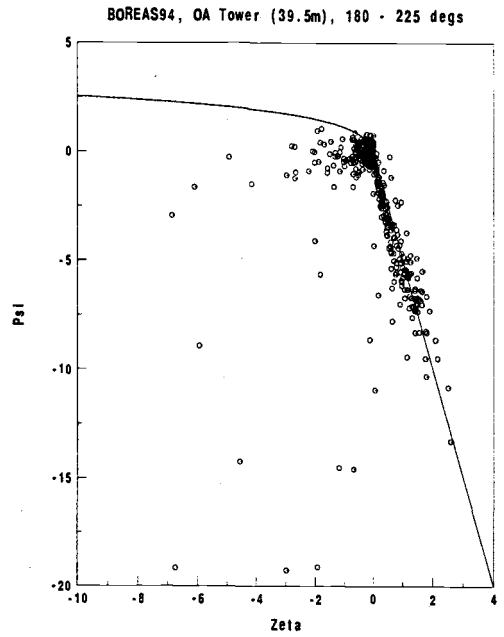

6a

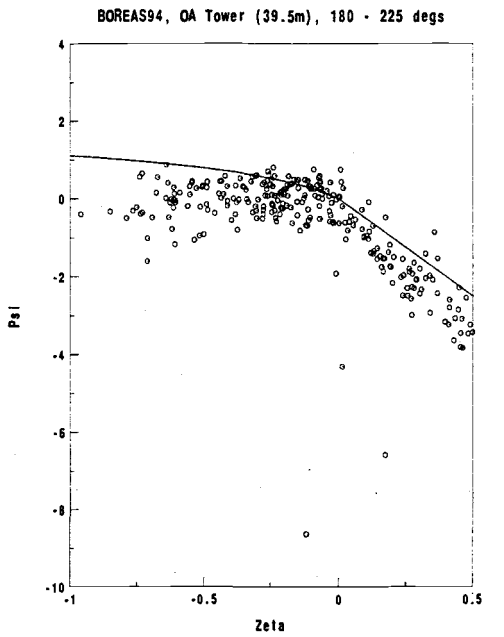

6b

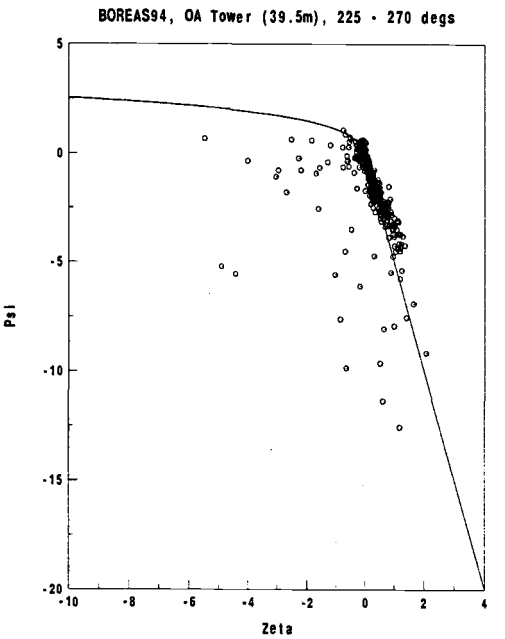

7a

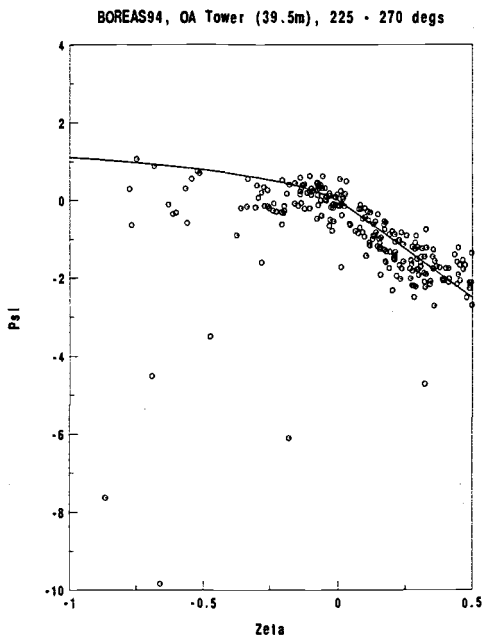

7b

Figure 6. Same as Figure 2 except for wind directions 180 - 225°.

Figure 7. Same as Figure 2 except for wind directions 225 - 270°.

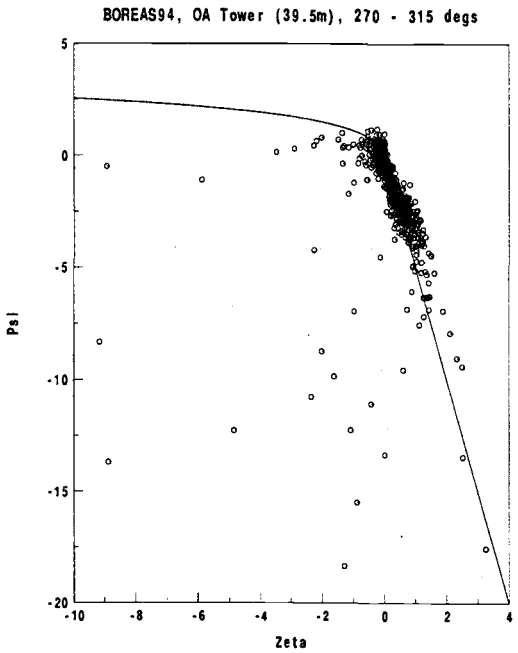

8a

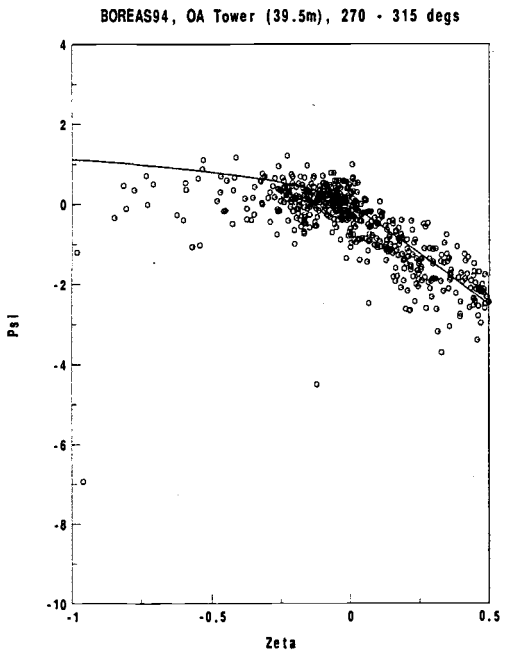

8b

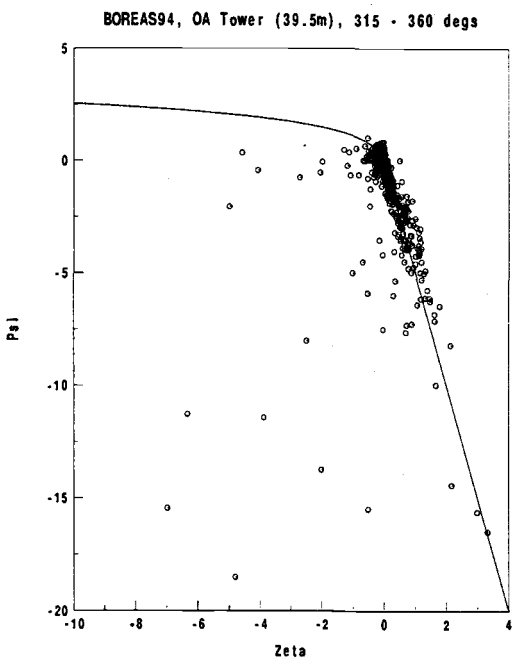

9a

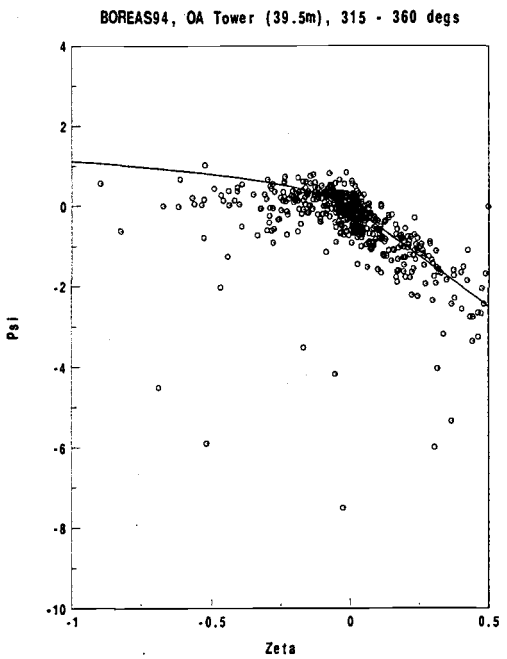

9b

Figure 8. Same as Figure 2 except for wind directions 270 – 315°.

Figure 9. Same as Figure 2 except for wind directions 315 – 360°.

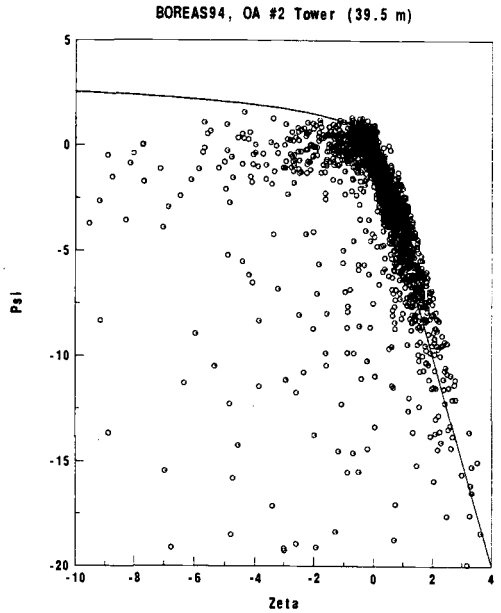

10a

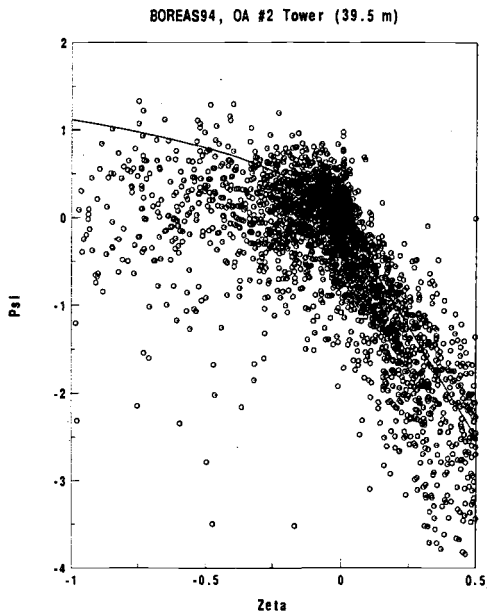

10b

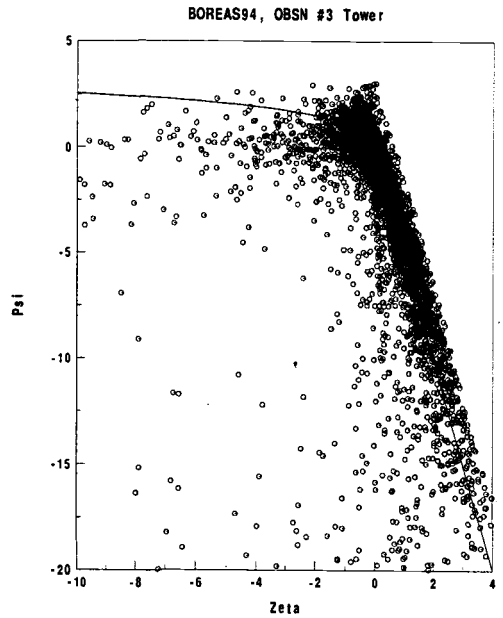

11a

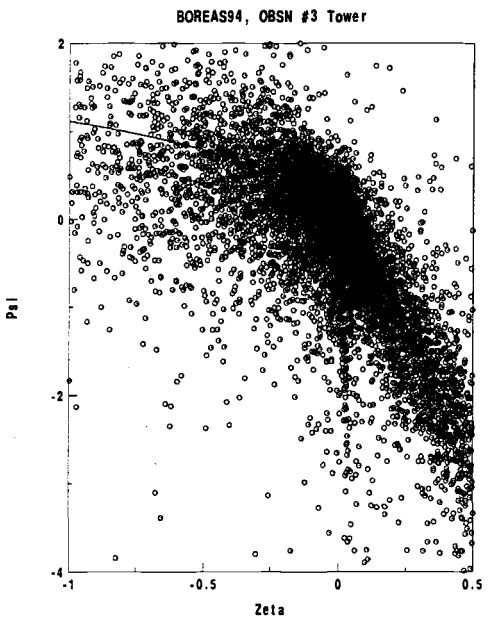

11b

Figure 10. Computed and predicted values of ψ plotted (dots and line, respectively) against the stability parameter ζ for all wind directions at the BOREAS Old Aspen site. 10b is an enlargement of 10a. Predicted values based on Paulson (1970) and Dyer (1974).

Figure 11. Same as Figure 10 except for BOREAS Black Spruce North site.

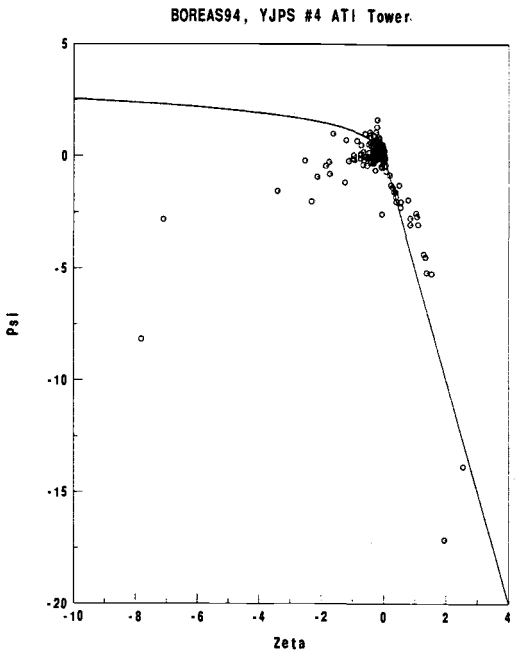

12a

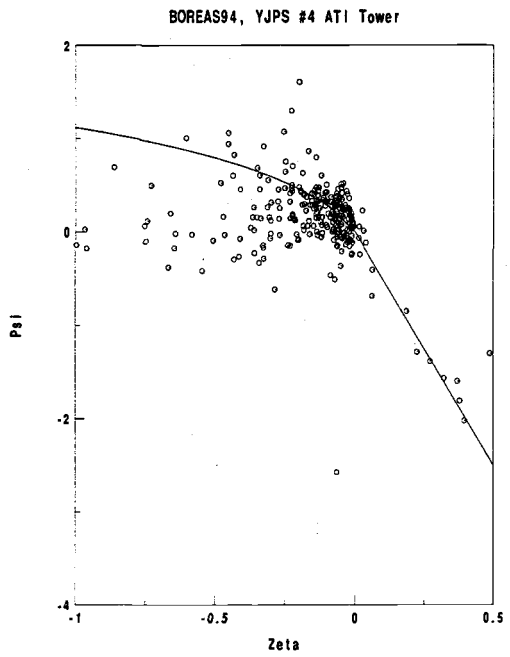

12b

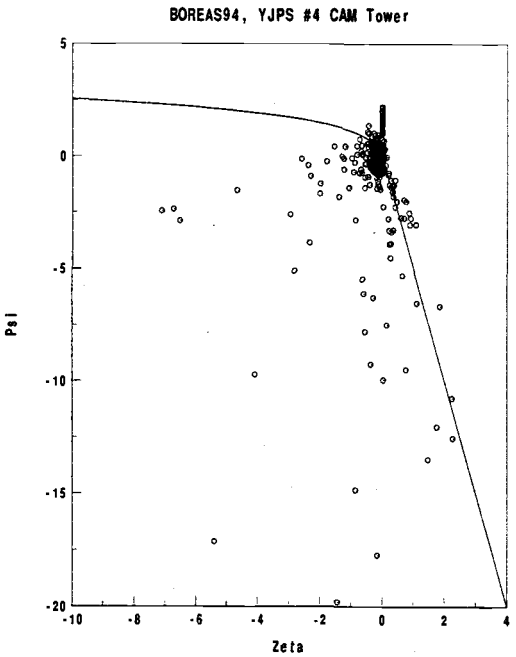

13a

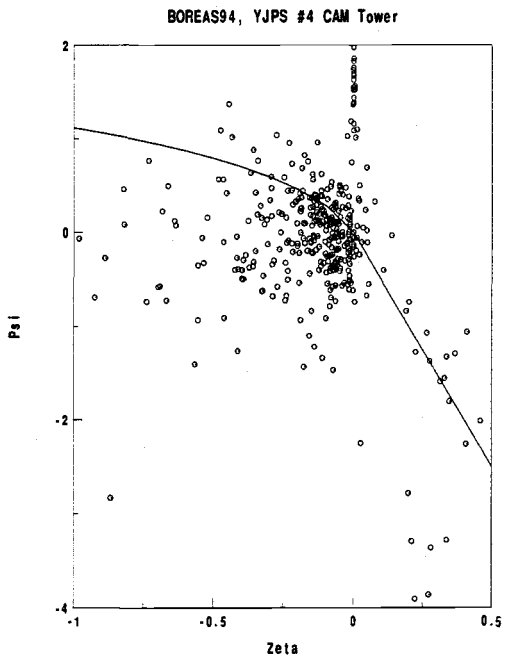

13b

Figure 12. Same as Figure 10 except for BOREAS Young Jack Pine South site (ATI).

Figure 13. Same as Figure 10 except for BOREAS Young Jack Pine South site (CAM)

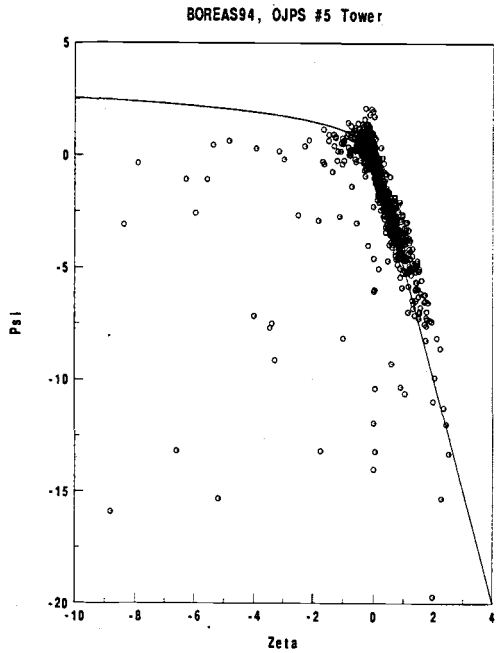

14a

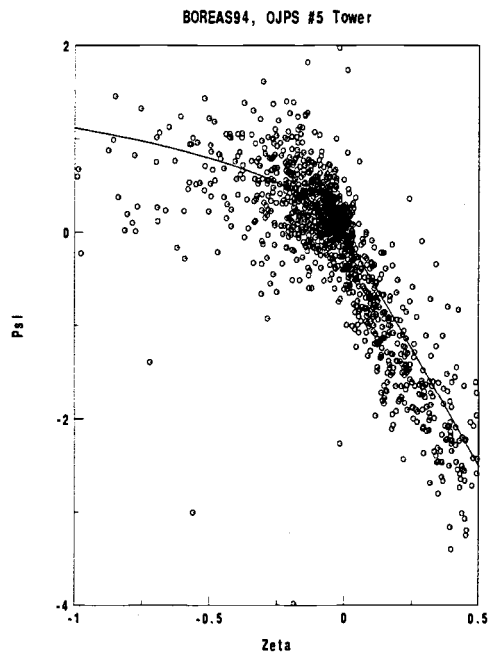

14b

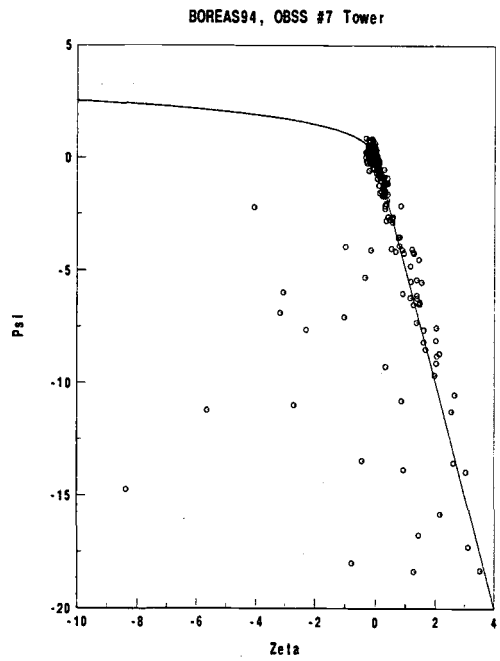

15a

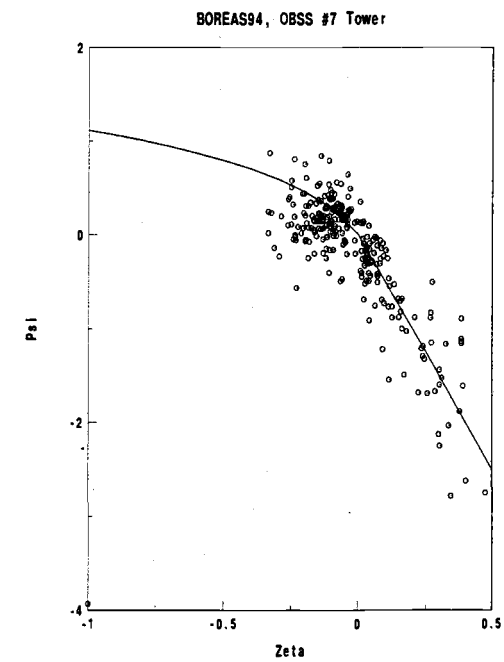

15b

Figure 14. Same as for Figure 10 except for BOREAS Old Jack Pine South site

Figure 15. Same as for Figure 10 except for BOREAS Old Black Spruce South site

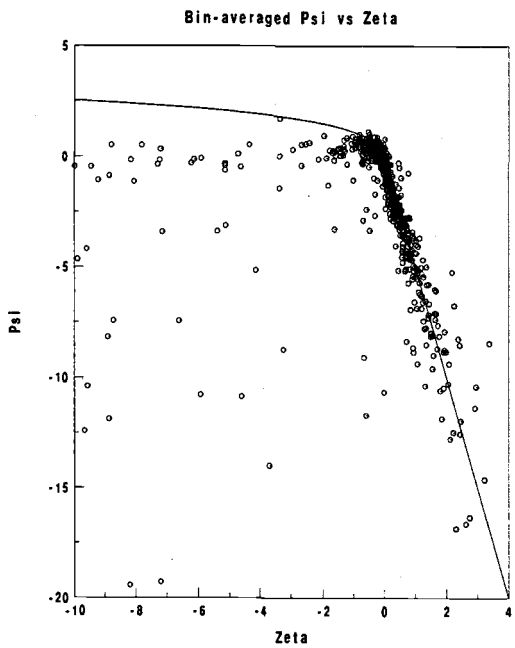

16a

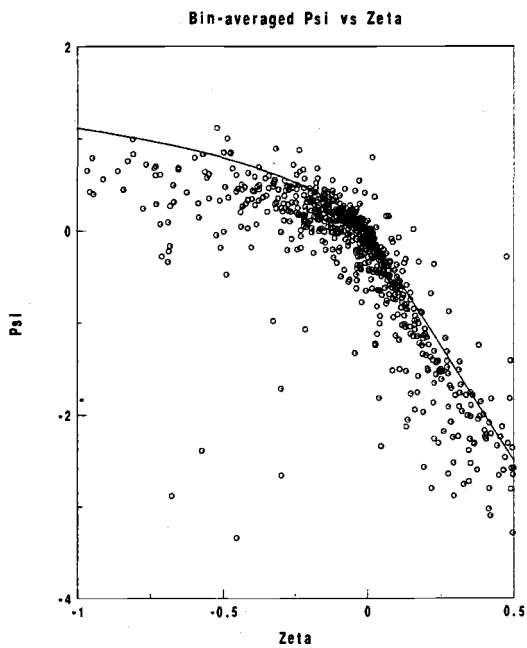

16b

Figure 16. Predicted values of ψ (line) and bin-averaged calculated values of ψ (dots) from all the BOREAS sites plotted against the stability parameter ζ. 16b is an enlargement of 16a.

predicted values of ψ agree less, but the agreement is much better than for the unstable case. This result implies that the M-O similarity theory with the Dyer-ψ function is able to predict the tower-based local momentum fluxes reasonably well for the stable case. Unlike the stable case, the ψ values predicted by Paulson-ψ-formulation in the unstable case are systematically larger than those observed by the towers. This is true for all the wind directions. The results for the OA site, for example, are shown in Figures 2-9 for the OA site, and for all BOREAS tower measurements (Figures 10 – 15). The computed values of ψ even tend to be negative in unstable conditions.

A different result is found for the fluxes measured at the Microfronts tower site located in grassland (Figures 17 and 18). The computed and predicted values of ψ match fairly well for unstable conditions at both levels without significant bias, although the scatter is large for the unstable case. For stable conditions, the computed values of ψ at the 3 m height are predicted well, and those at the 10 m height are systematically smaller than the predicted values of ψ by Dyer-ψ formulation. These observations indicate the likelihood that the 10 m height was above the surface layer at nighttime.

Consequently, the Dyer-ψ formulation is applicable to nocturnal tower flux measurements over forest canopies and grassland, provided the measurement height is in the surface layer, whereas the Paulson-ψ formulation is applicable to the daytime tower flux measurements over grassland but not over the forest canopies.

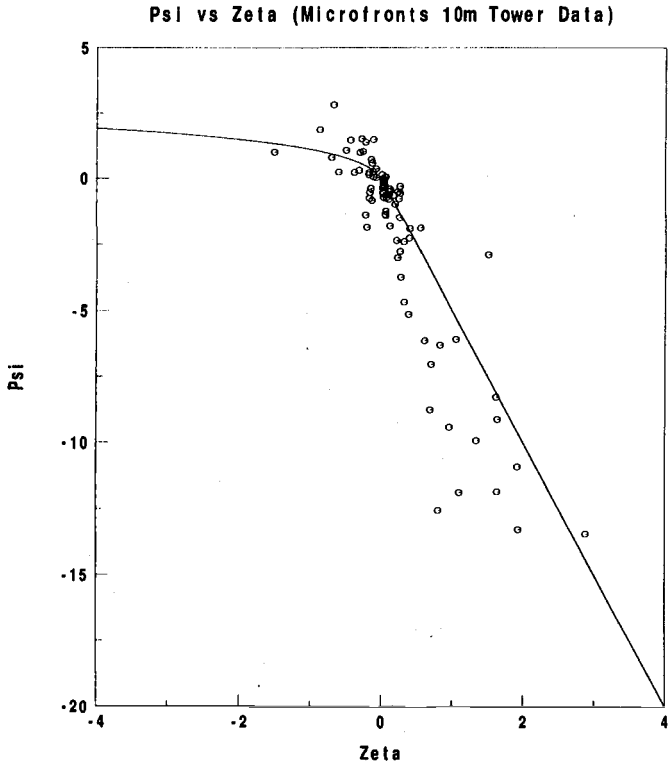

17

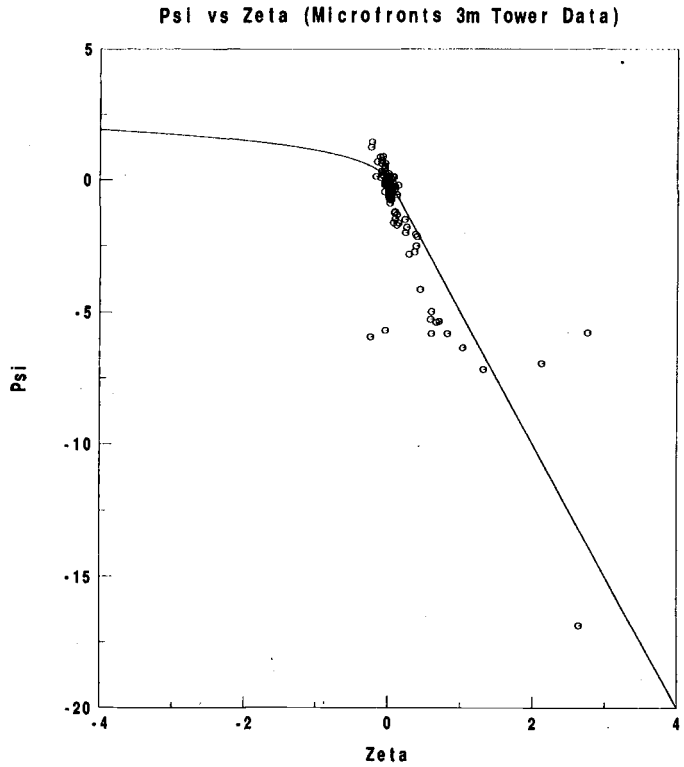

18

Figure 17. Computed and predicted values of ψ (dots and line, respectively) plotted against the stability ζ for grassland in Microfronts. The measurement height was 10 m.

Figure 18. Same as Figure 17 except for 3m.

These findings may be consistent with deep roughness sublayer effects over heated forest canopies. The roughness sublayer is the region adjacent to the surface where the time-averaged flow varies horizontally due to the influence of individual roughness elements. The roughness sublayer is thought to deepen with increasing instability as thermals anchored to individual roughness elements penetrate vertically. Chen and Schwerdtfeger (1989) observed deeper roughness sublayers with increasing instability. On the other hand, Raupach (1979) and Garratt (1980) did not find a dependence of the roughness sublayer depths on stability in unstable conditions.

In daytime heated conditions, the roughness sublayer may extend up above the turbulence measurement level on the towers over the forest, putting the flux measurements in the roughness sublayer and making M-O similarity theory inapplicable. This could explain the discrepancy between the observed and computed values of ψ.

Flow distortion due to the tower, boom or sonic transducers is not a likely cause of the disagreement between the tower observations and predicted values of ψ for BOREAS, since the disagreement is observed regardless of the wind direction and is not observed for nocturnal conditions.

6. Results for Aircraft Data Analyses

6.1 Area-Averaged Momentum Roughness Length

The area-averaged momentum roughness lengths computed from neutral conditions for BOREAS study sites and SGP El Reno flight track are summarized in Table 2. Note that both the area-averaged and local momentum roughness lengths are computed for BOREAS OA, OBSN and OBSS study sites. It is found that the local momentum roughness length based on the tower measurement is larger than the area-averaged momentum roughness length in these sites by 16-41 %. This may be associated with two related possibilities: 1) the aircraft was usually in the surface layer whereas the towers were mostly in the roughness sublayer as will be explained in more detail in Section 7.5. 2) the aircraft tracks often included some non-forested areas.

The area-averaged momentum roughness lengths of some BOREAS study sites seem to have changed significantly between 1994 and 1996. A possible explanation for this finding is that the number of flights in BOREAS 96 were smaller than in BOREAS 94, which yielded a smaller number of near-neutral flights to estimate the area-averaged momentum roughness length. Thus, the area-averaged momentum roughness lengths computed for BOREAS 96 are subject to more random errors than those for BOREAS 94. In fact, the largest temporal change in the area-averaged momentum roughness length is observed at YJPN, and

this study site had the least data in near-neutral conditions among the study sites both in BOREAS 94 and 96.

Table 2. Area-averaged momentum roughness lengths (z_{om}^{eff}) of BOREAS 94, BOREAS 96 and SGP study sites.

BOREAS 94 Study Sites	Flight Track (km)	Displacement Height d_o (m)	Range of ζ used for near-neutral conditions	Area-Averaged Momentum Roughness Length (z_{om}^{eff}) (m)
OA	12-13	11.5	$\zeta < -0.1$	1.9
OBSN	3	5.5	$\zeta < -0.1$	0.92
OBSS	20	7.2	$\zeta < -0.1$	0.79
Grid DE		4.7	$\zeta < -0.1$	0.87
Grid FG		4.7	$\zeta < -0.15$	1.3
OJPN	3	7.5	$\zeta < -0.1$	1.3
YJPN	3	3.0	$\zeta < -0.1$	0.37

BOREAS 96 Study Sites	Flight Track (km)	Displacement Height d_o (m)	Range of ζ used for near-neutral conditions	Area-Averaged Momentum Roughness Length (z_{om}^{eff}) (m)
OA	12-13	11.5	$\zeta < -0.1$	2.0
OBSN	3	5.5	$\zeta < -0.2$	1.2
OBSS	20	7.2	$\zeta < -0.1$	1.1
Grid DE		4.7	$\zeta < -0.1$	1.3
Grid FG		4.7	$\zeta < -0.15$	1.2
OJPN	3	7.5	$\zeta < -0.1$	1.3
YJPN	3	3.0	$\zeta < -0.1$	0.66

SGP El Reno Flight Track Aircraft	Flight Track (km)	Displacement Height d_o (m)	Range of ζ used	Area-Averaged Momentum Roughness Length (z_{om}^{eff}) (m)
Twin Otter	12	0	$\zeta < -0.1$	0.068
Long EZ	12	0	$\zeta < -0.1$	0.33
			$\zeta > -0.1$	0.10

6.2 Area-Averaged Momentum Roughness Length over the SGP Study Site

Figures 19 and 20 show the spatial series of momentum roughness lengths based on 1-km-averaged momentum fluxes over the SGP El Reno flight track computed from the Twin Otter and Long EZ data sets. These figures indicate that the momentum roughness length tends to be larger in the west and smaller in the east, which is related to the heterogeneous surface conditions. This result agrees with the fact that the western part contains more scattered trees and is less flat.

Similarly as in Mahrt and Ek (1993), the average of the individual momentum roughness lengths of 1-km-scale is found to be larger than the momentum roughness length based on fluxes averaged over the entire flight leg. Two methods for spatially averaging the momentum roughness lengths of 1-km-scale, logarithmic averaging and normal unweighted averaging, yield area-averaged momentum roughness lengths with very similar values. The small difference between the two averaging methods is probably associated with the relatively small spatial variation in the magnitude of the momentum roughness length over this particular flight track.

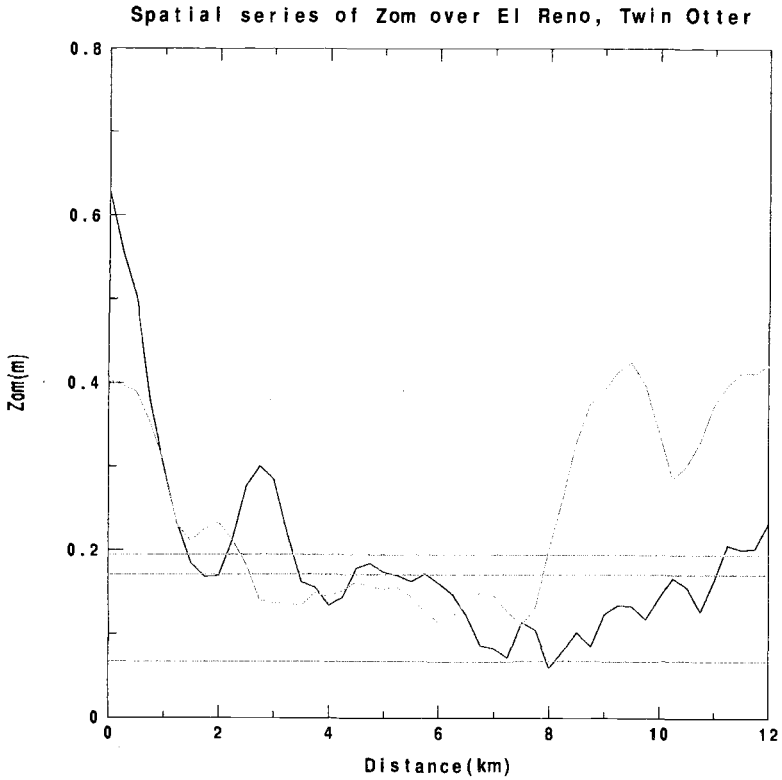

19

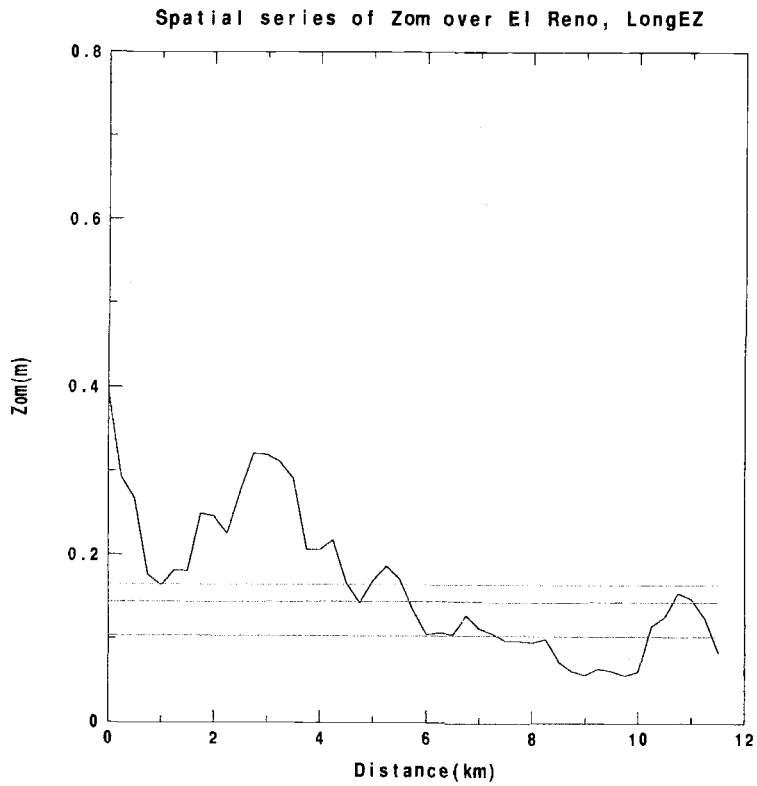

20

Figure 19. Area-averaged momentum roughness lengths for the SGP El Reno flight track based on Twin Otter Aircraft measurements. The black line is the spatial series of 1-km-averaged momentum roughness lengths. The red and green lines are the direct and logarithmic averages, respectively. The blue line is the area-averaged momentum roughness length of the entire flight track based on flux measurements from near-neutral flights only. The maroon line is the NDVI.

Figure 20. Same as Figure 19 except that the result is based on the Long EZ Aircraft measurements. NDVI not available for Long EZ data

6.3 Applicability of Paulson-ψ Formulation

As opposed to the tower data for unstable conditions, the computed values of ψ based on the area-averaged fluxes agree fairly well with the predicted values by the Paulson-ψ formulation over a large range of unstable conditions except for the case of SGP Long EZ (Figures 21 - 24). That is, the Paulson-ψ function is able to predict the area-averaged momentum flux over a weakly heterogeneous agricultural surface, given an area-averaged momentum roughness length estimated from near-neutral conditions.

The computed and predicted values of ψ are found to disagree in the analysis of the SGP Long EZ data. In this case, the computed values of ψ are based on the area-averaged momentum roughness length, z_{om} = 0.33 m, estimated from the fluxes sampled by a single Long EZ flight. In SGP, only one Long EZ flight flew in a near-neutral non-transitory boundary layer. The record shows that this particular flight took place between 0943 and 1140 local time. The boundary layer was likely well established for most of this time period.

From the other Long EZ flights flown in unstable conditions, M-O similarity theory with Paulson-ψ stability formulation consistently predicted $z_{om} \approx$ 0.1 m instead of z_{om} = 0.33 m. If the area-averaged momentum roughness length is set to z_{om} = 0.10 m, the simple average of the predicted area-averaged momentum roughness lengths for all flights except the neutral flight, then the

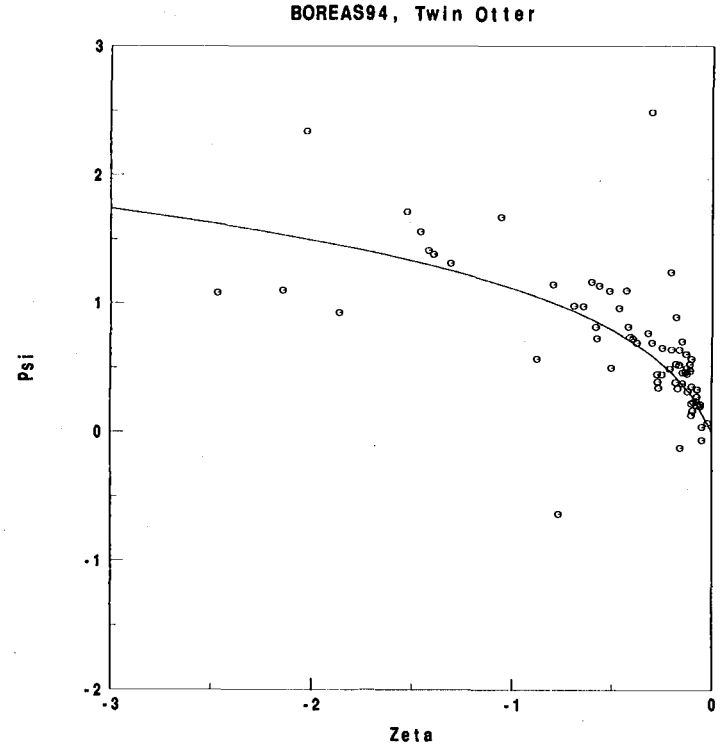

21

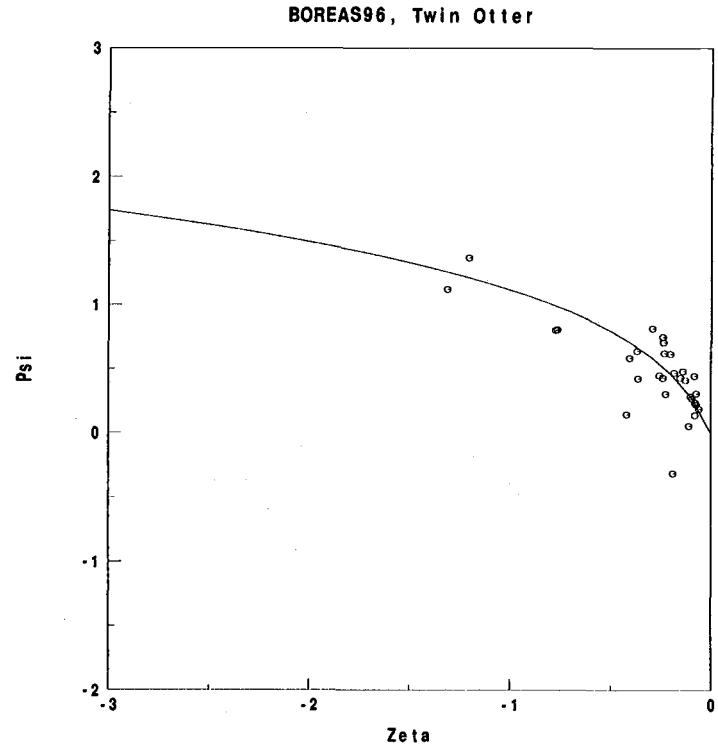

22

Figure 21. Computed and predicted values of ψ (dots and line, respectively) (Paulson, 1970 and Dyer, 1974) plotted against the stability parameter ζ, combined for all the BOREAS study sites. The result is based on flight-averaged fluxes measured by the Twin Otter Aircraft in BOREAS 94.

Figure 22. Same as Figure 22 except for BOREAS 96.

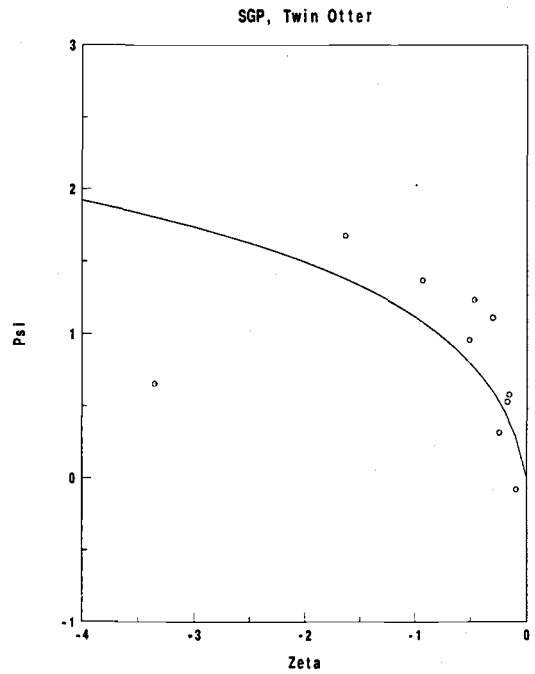

23

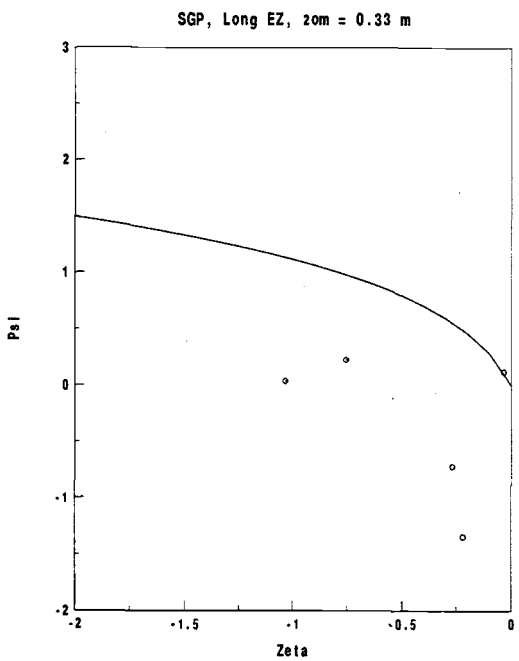

24

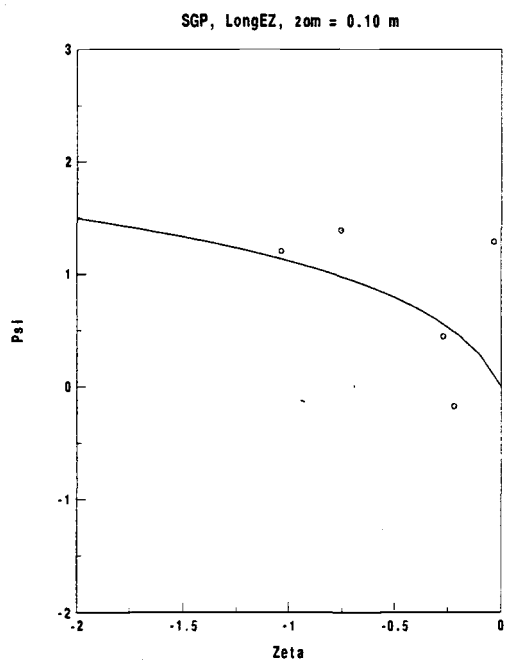

25

Figure 23. Same as Figure 22 except for SGP Twin Otter.

Figure 24. Same as Figure 22 except for SGP Long EZ. The area-averaged momentum roughness length is set to 0.33 m.

Figure 25. Same as Figure 24 except that the area-averaged momentum roughness length is set to 0.10 m

Paulson-ψ stability formulation gives a good fit to the computed values of ψ (Figure25). This finding and a result for the case of Twin Otter over the same flight track may imply sampling errors for the single Long EZ flight in near-neutral conditions rather than inapplicability of the Paulson-ψ formulation for predicting the area-averaged momentum fluxes.

7. Discussion

In the tower data analyses above, it was found that the Dyer-ψ formulation is applicable for predicting the tower-based momentum fluxes in stable conditions both over grassland and forest canopies, while the Paulson-ψ formulation is applicable only over grassland in unstable conditions. The computed values of ψ over the forest canopies are systematically smaller than the predicted values by the Paulson-ψ formulation. Surprisingly, however, the Paulson-ψ formulation is able to predict the area-averaged fluxes from the aircraft data including BOREAS aircraft data, where tower flux measurements made at the same time and level are not predicted correctly by the same formulation. For OA and OBSN, the measurement heights of aircraft and tower data were approximately at the same level.

It is possible that the flux measurements were made in the roughness sublayer at BOREAS tower sites in unstable conditions. In order to investigate this hypothesis, data from the Old Aspen study site in BOREAS 94 are examined in more detail. The aspen site is selected because 1) turbulence measurements took place at two levels, 28.1 m and 39.5 m, both above the forest canopy 2) the higher level of the turbulence measurements on the tower is roughly the same as the height of aircraft operation and 3) the OA site is considered to be one of the more homogeneous sites.

For investigating possible roughness sublayer effects on the OA tower measurements, the following three analyses are performed: 1) a comparison of the momentum roughness length and values of ψ between the 28.1m-level and 39.5m-level, 2) computation of the gradient of the mean wind speed and momentum fluxes between the two levels and 3) estimation of the roughness sublayer depth over the study site from existing formulations.

The properties of the roughness sublayer vary according to the size, spatial arrangement and density of the roughness elements. Despite the complexity, general features of the roughness sublayer have been investigated and formulated in the literature. However, the focus of these previous studies was always on point observations rather than horizontally averaged observations of properties. Horizontal averaging is necessary for studying the universal features of the roughness sublayer because of the horizontal heterogeneity on the scale of the roughness elements. As a result, no universal features of the roughness sublayer have been proven. Therefore, comparison of the results of the analyses from the OA tower presented below to those from earlier studies do not lead to definite conclusions.

7.1 Roughness Lengths and Values of ψ

The local momentum roughness length and computed values of ψ from the two levels of the OA tower are now compared. If both levels or at least the lower

level is in the roughness sublayer, the effects of the surface roughness elements are expected to be larger at the 28.1 m-level than at the 39.5m-level since the 28.1 m-level is closer to the canopy top. Table 3 shows the momentum roughness lengths computed for 8 wind directions from the 28.1 m-level compared against those from the 39.5 m-level reported in Table 1. The momentum roughness lengths computed for the 28.1 m-level differ from those computed for the 39.5m-level by as much as 56 %, indicating that the surface layer formulation is not applicable between the two levels. This result implies that at least the 28.1 m-level was in the roughness sublayer.

Table 3. Momentum roughness lengths of the BOREAS OA site computed from flux measurements at the 28.1 m-level in comparison to those at the 39.5 m-level reproduced from Table 1

Wind Direction	Momentum Roughness Lengths (m) z = 28.1 m, d_o = 11.5 m		Momentum Roughness Lengths (m) z = 39.5 m, d_o = 11.5 m	
	Daytime	Nighttime	Daytime	Nighttime
0 – 45 °	3.1	3.2	2.4	2.1
45 – 90 °	2.7	2.7	2.0	2.1
90 –135 °	3.0	3.2	2.3	2.5
135 – 180 °	2.6	2.6	1.7	1.8
180 – 225 °	2.9	2.5	2.4	2.1
225 – 270 °	3.0	2.9	2.6	2.6
270 – 315 °	2.8	2.4	2.0	1.7
315 – 360 °	3.2	3.2	2.6	2.4

Figure 26 illustrates computed values of ψ for the 28.1 m-level that can be compared to Figure 10. It is clear that the 28.1 m-level is less unstable than the

39.5 m-level overall. This observation agrees with the theory that shear production of turbulence is more predominant closer to the canopy top. At the 28.1 m-level, the computed values of ψ are also systematically smaller than the predicted values in unstable conditions as in the case of all the BOREAS towers (figures 10 – 15). Since it was concluded that the 28.1 m-level had been in the roughness sublayer from the roughness length computation, systematically smaller values of computed ψ compared to the values of predicted ψ in unstable conditions may be attributed to roughness sublayer effects in general. At the 39.5 m-level, the computed values of ψ show more scatter and sometimes much smaller values than the predicted values of ψ compared to the 28.1 m-level. On the other hand, some of the computed values of ψ at the 39.5 m-level are close to the predicted values, which may be due to situations where the 39.5-m level was in and out of the roughness sublayer. However, these observations are not spatially averaged and the difference between the two levels may be due to the change of footprint with height, which is expected to be important in the roughness sublayer.

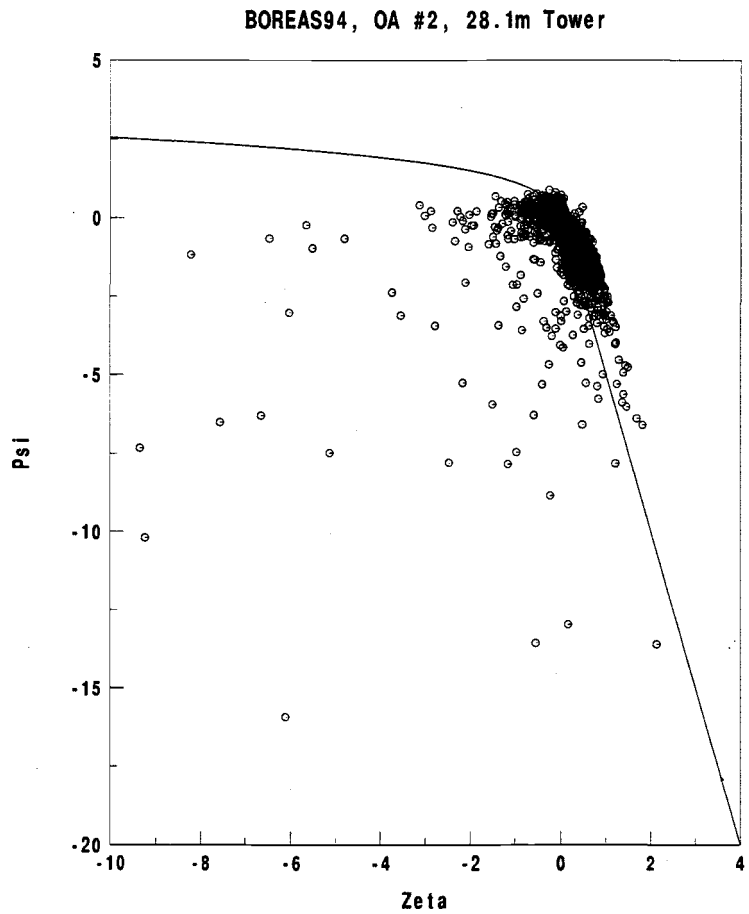

Figure 26. Computed and predicted values of ψ (dots and line, respectively) plotted against the stability parameter ζ for all the wind directions of the BOREAS Old Aspen site. The measurement height was 28.1m. Predicted values based on Paulson (1970) and Dyer (1974).

7.2 Gradients of Mean Wind and Momentum Fluxes

Integrating (3) from U_1 to U_2 and from z_1 to z_2 in the surface layer, we obtain

$$U_2 - U_1 = \frac{u^*}{\kappa}\left[\ln\left(\frac{z_2}{z_1}\right) - \psi(\zeta_2) + \psi(\zeta_1)\right] \qquad (7)$$

where ζ_1 and ζ_2 correspond to ζ at levels z_1 and z_2. If it is assumed that the two levels of the OA tower measurements were made in the surface layer, then in unstable conditions, equation (7) with the ψ formulation by Paulson (1970) can be applied to predict the difference in wind speed or mean wind gradient between these levels. The predicted wind gradient can be then compared to the observed wind gradient for all unstable conditions (Figure 27) and for near-neutral conditions only ($-0.03 < \zeta < 0$) to eliminate the possible problems of using an incorrect ψ formulation (Figure 28). Figures 27 and 28 indicate that the observed mean wind gradient is larger than the mean wind gradient predicted by the surface layer formulation.

As opposed to our result, wind gradients in the entire roughness sublayer, for a given flux, have been observed to be weaker than M-O similarity theory would predict in the surface layer (Garratt, 1980). Fazu and Schwerdtfeger (1989)

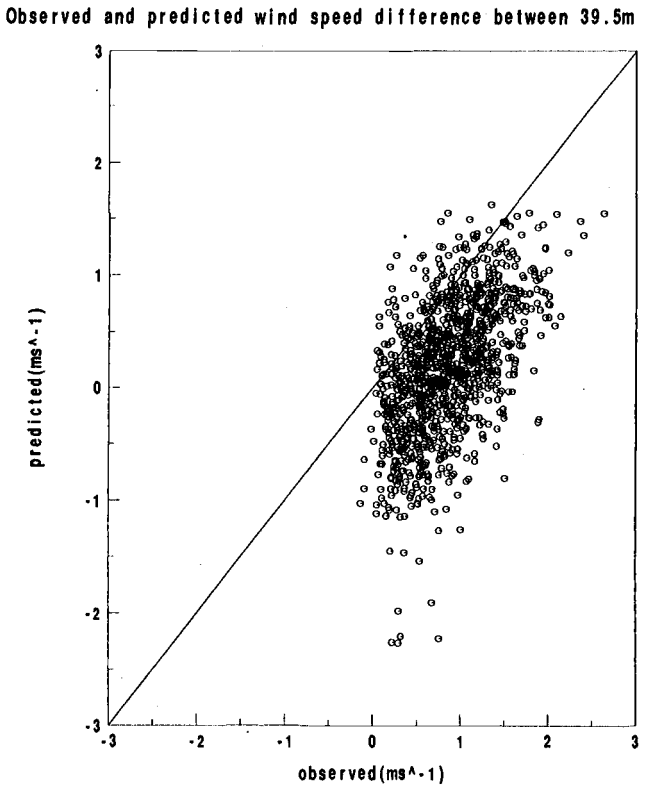

27

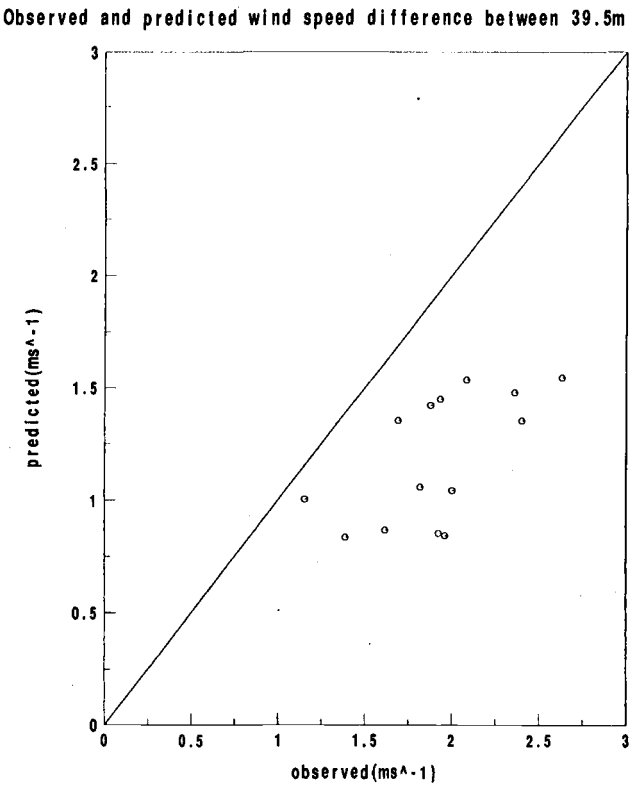

28

Figure 27. Comparison of the observed and predicted wind speed differences between 39.5-m- and 28.5-m-levels on the BOREAS OA tower. The predicted wind speed difference is based on equation (7). The black line in the figure indicates the 1:1 line

Figure 28. Same as Figure 27 except only from near-neutral conditions. (Note the different scales.)

observed the same for the lower roughness sublayer, but the wind gradient was larger in the upper roughness sublayer. Mulhearn and Finnigan (1978) showed considerable spatial variations of the mean wind profiles near the roughness elements in their wind-tunnel experiments.

Figures 29 and 30 compare daytime to nighttime friction velocities at 39.5 m and 28.1 m. The ratio of the friction velocity between the two heights is greater on average during the nighttime, however, the scatter of the ratio is also greater during the nighttime than during the daytime. The more rapid decrease of the friction velocity with height at night may be attributable to thin nocturnal boundary layers. In addition, the friction velocity is small at night and may be subject to more significant flux errors.

The observed 15% – 25% decrease in the friction velocity over a height difference of 10m, would cause a significant deceleration of the mean wind speed. The observed vertical gradient of the momentum flux acting alone would cause $0.01 m/s^2$ and $0.005 m/s^2$ deceleration of the mean wind speed on average for the daytime and nighttime periods, respectively. A mean wind field of 5 m/s would cease after 8.5 minutes for the daytime and 17 minutes for the nighttime. In addition, such a large vertical flux divergence implies a difference of ~100m/s between the geostrophic wind speed and the mean wind speed in the boundary layer. Therefore, it is unlikely that the calculated values are the actual vertical divergence of the momentum flux over a significant horizontal area. Such a large

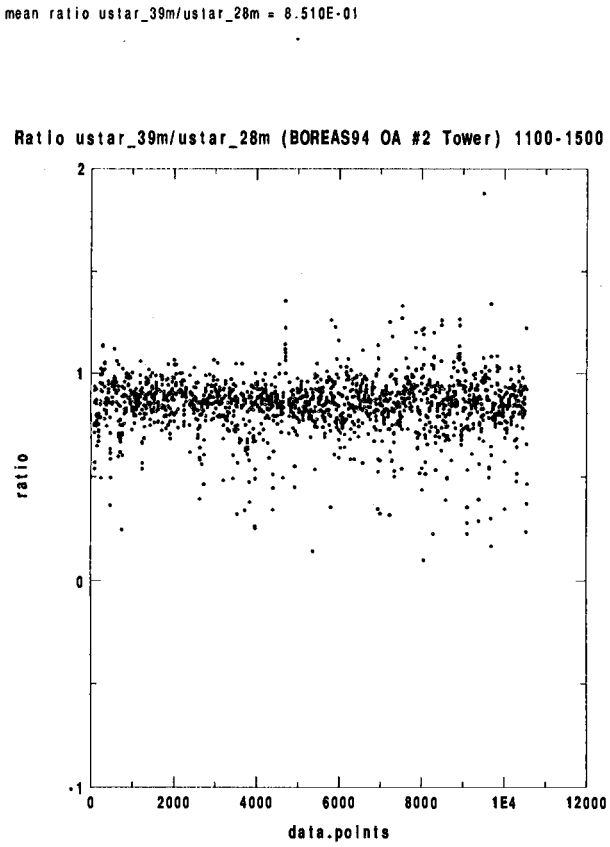

29

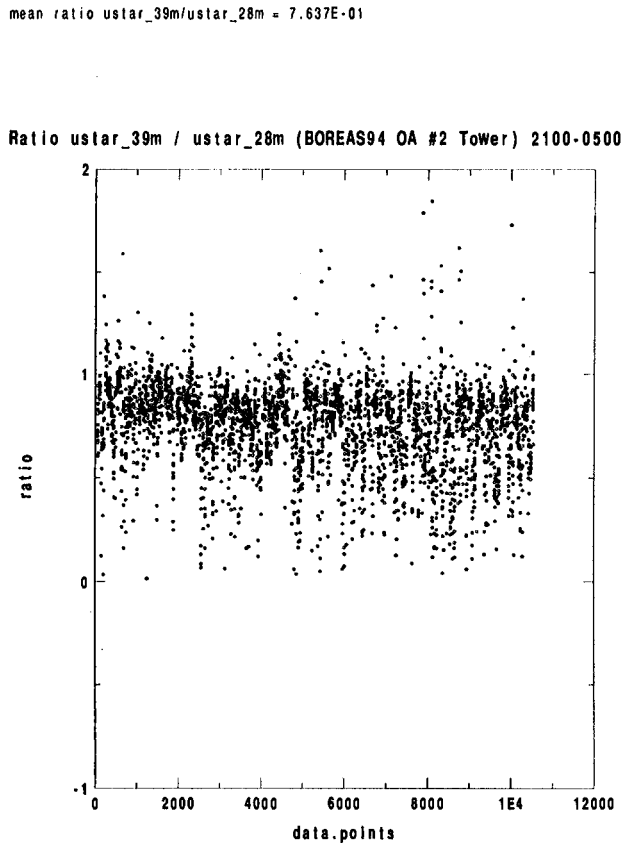

30

Figure 29. The ratio of the friction velocity at 39.5 m to that at 28.1 m for the BOREAS OA tower during the daytime (1100-1500 local).

Figure 30. Same as Figure 29 except for the nighttime (2100 – 0500 local).

difference in momentum flux between the two levels may be explained by a change of footprint with height, which is expected in the roughness layer.

7.3 Roughness Sublayer Depth

The depth of the roughness sublayer over the OA forest canopy is now estimated using existing formulations in the literature. It is known that the depth of the roughness sublayer over a rough surface depends on the surface characteristics that may include the mean element spacing and the element width. Surface types are sometimes classified in terms the roughness concentration, λ, defined as the total roughness frontal area per unit horizontal area,

$$\lambda = \frac{lh}{\delta^2}$$

where l is the mean cross-stream element width, h is the mean roughness element height and δ is the mean spacing between elements. In general, the larger λ the more densely packed the roughness elements.

Tennekes (1973) predicted that the height of the roughness sublayer should be 100 times the momentum roughness length using theoretical explanations. Therefore, Tennekes (1973) suspected that the surface layer would not be present over very rough terrain. Garratt (1980) reported the ratio of the height of the roughness sublayer to the momentum roughness length (z^*/z_{om}) to be 150 and 35

for less dense (z_{om} = 0.4 m, λ = 0.03) and denser (z_{om} = 0.9 m, λ = 0.2) savannah. Garratt (1980) speculated that this ratio would decrease to about 10 for high density vegetation. Fazu and Schwerdtfeger (1989) found $z^*/z_{om} \approx$ 53 for bushland (z_{om} = 0.435 m, λ = 0.32).

The depth of the roughness sublayer has also been related to the mean spacing or inter-row spacing, z^*/δ (Garratt, 1980; Chen and Schwerdtfeger, 1989; Cellier and Brunnett,1992). Table 4 shows a summary of some of the roughness sublayer depths in relation to the surface characteristics given in the literature.

Table 5 shows the canopy architecture of the BOREAS study sites. The canopy characteristics of the OA site do not strictly resemble those of any sites studied earlier in the literature. Thus, an accurate estimation of the roughness sublayer depth over the OA site is difficult. Table 4 indicates that the possible depth of the roughness sublayer varies between 35 and 150 times the momentum roughness length above the displacement height of a rough surface. This formulation will yield a roughness sublayer depth of 77 to 330 m for the OA site (d_o = 11.5 m, z_{om} = 2.2 m). Using the formulations with mean spacing of elements z^*/δ, the roughness sublayer depth of the OA site (δ = 3.2 m) falls in the range of 3.6 and 15 m. It is obvious that the roughness sublayer heights estimated with the momentum roughness length and the mean spacing of elements differ from each other significantly, which may imply very different surface conditions of the OA site from the sites studied in the literature.

Table 4. Canopy architecture and depth of the roughness sublayer.

Canopy	Wind Tunnel, coarse gravel (Mulhearn and Finnigan, 1978)	Savannah I (Garratt, 1978, 1980)	Savannah II (Garratt, 1978, 1980)	Pine (Raupach, 1979)
h (m)	0.0012	8.0	9.5	16.6
δ (m)	0.047	20	10	3.2
l (m)	0.0145	1.5	2.0	2
λ	0.0787 ✻	0.03	0.2	3.1
z_{om} (m)	0.00038	0.4	0.9	0.9
z^*/z_{om}	132 ✻	150	35	10◆
z^*/δ	1.063 ✻	3	3	3◆
Canopy	Pine (Denmead and Bradley, 1985)	Sugar cane (Cellier, 1986)	Bushland (Fazu and Schwerdtfeger. 1989)	Maize crop (Cellier and Brunnet, 1992)
h (m)	16	3	2.3	2.35
δ (m)	3.8	1.6 ✻	5.0	0.8
l (m)	2	2.56 ✻	3.5	0.46 ✻
λ	2.2	3	0.32	1.7
z_{om} (m)	0.8		0.435	
z^*/z_{om}			53	
z^*/δ		3.1 ✣	4.6	3-4

h – mean height of elements
δ - mean distance between elements
l – mean diameters of elements
λ – roughness concentration
✻- calculated from the given data in the literature
◆- value implied by Garratt (1980) in his analysis of the pine forest studied by Raupach (1979)
✣- value reported in Cellier and Brunet (1992)

Table 5. BOREAS canopy architecture.

Site	OA (Tower #2)	OBSN (Tower #3)	YJPS (Tower #4)	OJPS (Tower #5)	OBSS (Towers #7)
h (m)	17.25	8.25	4.5	13.4	10.8
δ (m)	3.2	1.4	0.97	2.9	1.3
l (m)	0.205	0.085	0.032	0.129	0.071
λ	0.35	0.38	0.15	0.21	0.45
z_{om} (m)	2.2	1.3	0.64 (ATI) 0.79 (CAM)	1.1	0.68

z_{om} – averaged momentum roughness lengths for daytime and nighttime periods and all 8 wind direction groups.

The above estimation of the possible range of the roughness sublayer height over the OA site looked only at the overall range of possibilities. However, this estimation can be refined by examining the details of the canopy architecture. If the mean roughness element height and the roughness concentration of the OA site are considered, then the classification of the vegetation at the OA site should be situated somewhere between the denser savannah studied by Garratt (1980) and the pine forest studied by Raupach (1979).

In Garratt (1980), $z^*/z_{om} \approx$ 10 is inferred for the roughness sublayer depth of the pine forest studied in Raupach (1979). Given the momentum roughness length of 2.2 m estimated for the OA site, the roughness sublayer depth for the OA site would be between 22 ($z^*/z_{om} \approx$ 10) and 77 m ($z^*/z_{om} \approx$ 35). Since the ratio z^*/δ is approximately 3 for both the savannah and pine forest, the roughness

sublayer depth for the OA site (δ = 3.2m) would accordingly be 9.6m. Consequently, the reasonable range of the roughness sublayer depth over the OA site is between 9.6 and 77 m, and this is the best estimate possible with the existing literature.

Since the estimated displacement height of the OA site is 11.5 m, a roughness sublayer depth of at least 16.6 m and 28 m would put the sensor heights of 28.1 m and 39.5 m on the OA tower in the roughness sublayer, respectively. Thus, both measurement heights were probably in the roughness sublayer.

7.4 Comparison with Microfronts Tower Flux Measurements

For comparison with the BOREAS tower cases, M-O similarity theory with Paulson-ψ and Dyer-ψ formulations are evaluated for Microfronts tower flux measurements. As reported in Section 5.2, for the Microfronts study site, the Paulson-ψ formulation is able to predict the magnitudes of tower-based momentum fluxes for unstable conditions. This shows that M-O similarity theory and the Paulson-ψ formulation do work reasonably well even for tower-based fluxes in unstable daytime conditions.

The surface surrounding the tower in Microfronts was covered by grass, with a roughness length of only 0.015 m. With this small roughness length, the roughness sublayer would extend up to only 2.250 m (Garratt, 1978 and 1980) which is the largest estimate according to existing formulations in unstable

conditions. By any estimate, the sensor heights at 3 m and 10 m were well above the roughness sublayer. This finding supports the hypothesis that the BOREAS tower measurements were in the roughness sublayer.

7.5 Summary

The investigations above seem to indicate that even the highest tower levels were in the roughness sublayer over BOREAS forest canopies in unstable conditions. At the same time, the Paulson-ψ formulation succeeded in predicting the aircraft-measured fluxes, but failed to predict the tower-measured fluxes even when they were at the same level as the aircraft.

It is important to realize that eddies captured by the tower and aircraft have naturally different footprints even if both the tower and aircraft measurements were made at the same level in the same study site. Yet, it is still reasonable to suspect that the aircraft would have been in the roughness sublayer if the tower measurement had been in the roughness sublayer at these study sites. It is possible that the wind and flux observations at a fixed point on a tower in the roughness sublayer might not be representative due to the spatial preference of wakes and thermals attached to canopy elements and the very small footprint of eddies. Towers are sometimes erected in microscale clearings, which augments the effect of the roughness sublayer. Towers are sometimes located in drier locations with correspondingly more vigorous thermals and deeper roughness sublayers compared

to the average for a larger area on the scale of the aircraft track. This possibility might explain the success of the Paulson-ψ formulation for aircraft-measured area-averaged values and the failure of tower-measured values at the same height. Perhaps, the aircraft fly in the surface layer for most of the time and encounter the roughness sublayer only occasionally, thus the roughness sublayer effect becomes less important for flight-averaged fluxes.

Continuing this speculation, the greater success of the aircraft measurements may be due to partial cancellation of the variable roughness sublayer effects by area-averaging variables. With this argument, the deviation from M-O similarity theory is greater for point measurements than for spatially averaged variables.

One might suspect that the momentum roughness lengths computed with flux measurements made in the roughness sublayer with M-O similarity theory may be significantly different from the actual momentum roughness lengths. In the appendix of Garratt (1980), this issue was examined. The actual flux measurements in the roughness sublayer over a tree-covered surface were applied to an empirical flux-gradient relationship for roughness sublayers to compute the momentum roughness length. The result shows that the use of M-O similarity theory in the roughness sublayer to calculate the momentum roughness length involves only very small errors. Therefore, the roughness lengths estimated in the present study should not differ from the actual roughness lengths significantly even if the flux measurements took place in the roughness sublayer.

8. Conclusions

A number of tower and aircraft data sets collected over weakly heterogeneous forest canopies, agricultural fields and grassland are analyzed. Using M-O similarity theory, the local momentum roughness lengths for these study sites are computed with local flux measurements from towers in near-neutral conditions. Similarly, the area-averaged momentum roughness lengths are computed with area-averaged flux measurements from aircraft for near-neutral conditions. Simultaneous tower and aircraft flux measurements took place for some of the BOREAS study sites. At these sites, the local momentum roughness lengths are larger than the area-averaged momentum roughness lengths by 16-41%.

As a part of the investigation of the area-averaged momentum roughness length, a spatial series of 1-km-averaged momentum roughness lengths over a heterogeneous agricultural field is computed. The result shows variability in the magnitude of the momentum roughness length, associated with the surface heterogeneity. The area-averaged momentum roughness of the region based on the flight averaged fluxes is found to be smaller than that based on the individual 1-km-averaged momentum roughness lengths, as also observed in Mahrt and Ek (1993).

The data analysis shows that the Dyer ψ-formulation is able to predict the local fluxes measured on towers over forest canopies and grass in stable conditions

(provided the measurement height is the surface layer). The Paulson ψ-formulation is able to predict the tower-based fluxes over grass in unstable conditions but not over the forest canopies. Surprisingly, the Paulson-ψ formulation is able to predict the area-averaged fluxes measured by the aircraft for unstable conditions over the forest canopies. Figure 31 is a summary of the predicted and computed values of ψ with all the data analyzed in the present study. In the figure, the computed values of ψ for the Microfronts tower and those for the BOERAS towers are bin-averaged values to show the trend of computed values of ψ more clearly.

Despite the uncertainties, it remains likely that the tower measurements over forest canopies in BOREAS were made in the roughness sublayer during the daytime. The agreement of the nighttime measurements to the surface layer formulations suggest that the breakdown of the M-O similarity theory for the daytime measurements is due to deeper daytime roughness sublayer for unstable conditions. It is plausible that towers were sometimes in drier and warmer locations where the roughness sublayer is locally deeper. The greater success of the aircraft measurements may also be due to partial cancellation of the variable roughness sublayer effects by area-averaging variables.

Finally, it is recommended that in future experiments field tower measurements over forests should be made at higher levels to capture a larger footprint, that is they should be made above the roughness sublayer in the surface layer.

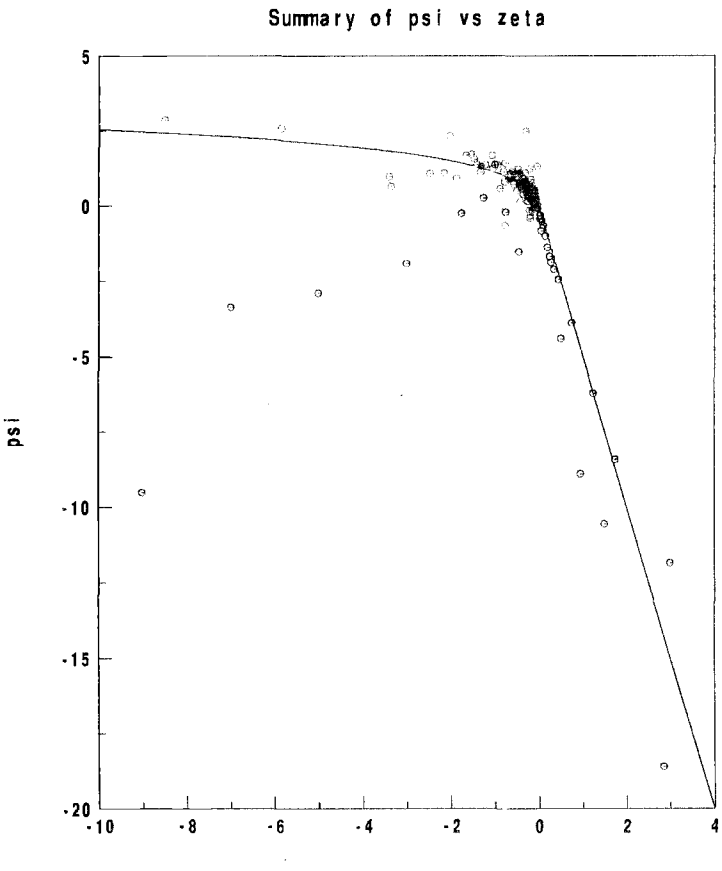

31a

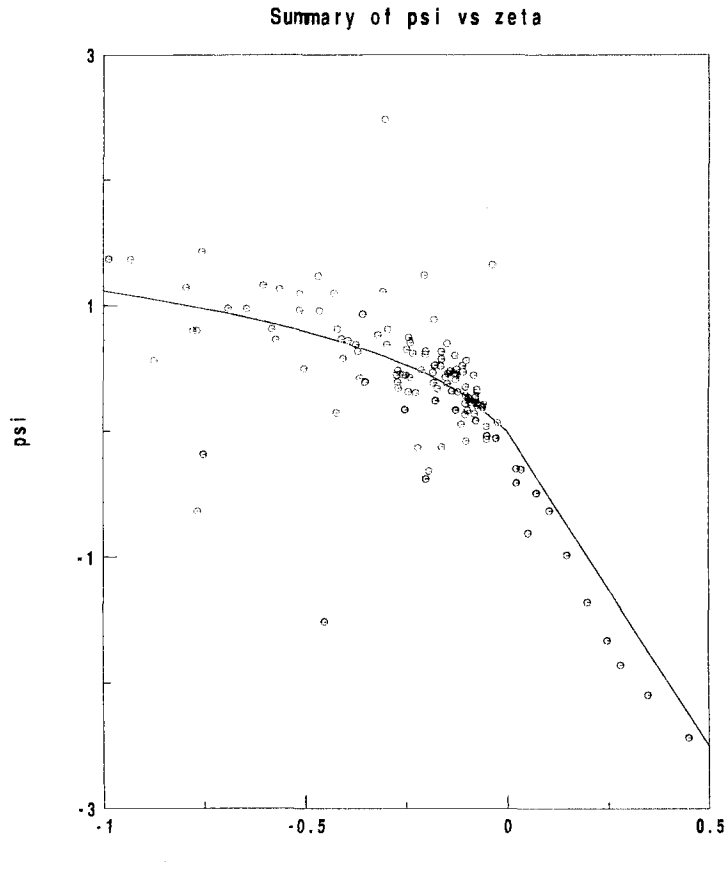

31b

Figure 31. Summary plot of ψ vs. ζ computed from BOREAS 94, BOREAS 96 and SGP aircraft data (red dots), BOREAS towers (bin-averaged, green dots) and Microfronts tower (bin-averaged, blue dots). The black line is the predicted values of ψ by Paulson (1970) and Dyer (1974) for unstable and stable conditions, respectively. 31b is an enlargement of 31a.

Bibliography

Cellier, P., 1986: On the validity of flux-gradient relationships above very rough surfaces. *Boundary-Layer Meteorol.* 36:417-419.

Cellier, P. and Y. Brunet, 1992: Flux-gradient relationships above tall plant canopies. *Agric. For. Meteorol.* 58:93-117.

Claussen, M., 1990: Area-averaging of surface fluxes in a neutrally stratified, horizontally inhomogeneous atmospheric boundary layer. *Atmos. Environ.* 24A:1349-1360.

Dyer, A.J., 1974: A review of flux-profile relationships. *Boundary Layer Meteorol.* 7:363-372.

Dyer, A.J. and B.B. Hicks, 1970: Flux-gradient relationships in the constant flux layer. *Quart. J. Roy. Meteorol. Soc.* 96:715-721.

Denmead, O.T. and E.F. Bradley, 1985: 'Flux-gradient relationships in a forest canopy' Pp. 421-442 in *The forest-atmosphere interaction.* Eds. Hutchinson, B.A. and Hicks, B.B.D. Reidel.

Fazu, C. and P. Schwerdtfeger, 1989: Flux-gradient for momentum and heat over a rough neutral surface. *Quart. J. Roy. Meteorol.* 115:335-352.

Garratt, J.R., 1978: Flux profile relations above tall vegetation. *Quart. J. Roy. Meteorol.* 104:199-211.

Garratt, J.R., 1980: Surface influence upon vertical profiles in the atmospheric near-surface layer. *Quart. J. Roy. Meteorol.* 106:803-819.

Goode, K. and S.E. Belcher, 1999: On the parameterisation of the effective roughness length for momentum transfer over heterogeneous terrain (Manuscript).

Högström, U., 1988: Non-dimensional wind and temperature profiles in the atmospheric surface layer: a re-evaluation. *Boundary-Layer Meteorol.* 42:55-78.

Mahrt, L. and M. Ek, 1993: Spatial variability of turbulent fluxes and roughness lengths in Hapex-Mobilhy. *Boundary-Layer Meteorol.* 65:381-400.

Mason, P.J., 1988: The formation of areally-averaged roughness lengths. *Quart. J. Roy. Meteorol.* 114:399-420.

Mulhearn, P.J. and J.J. Finnigan, 1978: Turbulent flow over rough, random surface. *Boundary-Layer Meteorol.* 15:109-132.

Panofsky. H.A., 1963: Determination of stress from wind and temperature measurements. *Quart. J. Roy. Meteorol.* 89:85-94.

Paulson, C.A., 1970: The mathematical representation of wind speed and temperature profiles in the unstable atmospheric surface. *J. Appl. Meteor.* 9:857-861.

Physick, W.L. and J.R. Garratt, 1996: Incorporation of a high-roughness lower boundary into a mesoscale model for studies of dry deposition over complex terrain. *Boundary-Layer Meteorol.* 74:55-71.

Raupach, M.R., 1979: Anomalies in flux-gradient relationships over forest. *Boundary-Layer Meteorol.* 16:467-486.

Sellers, P.J., F.G. Hall, J. Chihlar, P. Crill, D. Hartog, B. Goodison, R.D. Kelly, D. Lettenmeier, H. Margolis, J. Ranson and M. Ryan (Eds), 1994: BOREAS Experiment Plan Chapters 1 – 3.

Sellers, P.J., F.G. Hall, R.D. Kelly, A. Black, D. Baldocchi, J. Berry, M. Ryan, K.J. Ranson, P.M. Crill, D.P. Lettenmeier, H. Margolis, J. Cihlar, J. Newcomer, D. Fitzjarrald, P.G. Jarvis, S.T. Gower, D. Halliwell, D. Williams, B. Goodison, D.E. Wickland and F.E. Guertin, 1994: BOREAS in 1997: Experiment overview, scientific results, and future directions. *J. Geophys. Res.* 102:28731-28769.

Sun, J.: Diurnal variations of thermal roughness height over a grassland (to appear in *Boundary-Layer Meteorol.*).

Taylor, P.A., 1987: Comments and further analysis on effective roughness lengths for use in numerical three-dimensional models. *Boundary-Layer Meteorol.* 39:403-418.

Tennekes. H., 1973: The logarithmic wind profile. *J. Atmos. Sci.* 30:234-238.

Vickers, D., 1999: Drag over forest canopies. BLG report. College of Oceanic and Atmospheric Sciences, Oregon State University.

Vickers, D. and L. Mahrt, 1997: Quality control and flux sampling problems for tower and aircraft data. *J. Atm. Oc. Tech.* 14: 512-526.

Appendices

Appendix 1: Variables in Equation (4)

Equation (4) contains a number of variables including those measured directly and those computed from the measured values. This section illustrates how all the variables in equation (4) are obtained.

With the displacement height, equation (4) is written as

$$U = \frac{u^*}{\kappa}\left[\ln\left(\frac{z-d_o}{z_{om}}\right) - \psi(\zeta)\right] \tag{4}$$

The known variables measured directly are the wind speed U, the friction velocity u^*, the von Karman constant κ, the height above the ground z, the displacement height d_o, and the stability parameter ζ.

The wind speed U is computed from the equation

$$U = \sqrt{u^2 + v^2}$$

where u and v indicate the measured wind velocity of the rotated x- and -y coordinates respectively.

As in section 2.1, the friction velocity u^* is defined as

$$u^* \equiv \sqrt[4]{\overline{u'w'_s}^2 + \overline{v'w'_s}^2}$$

and computed from the surface values of the vertical momentum fluxes $\overline{u'w'_s}$ $\overline{v'w'_s}$ measured by the eddy-correlation system.

The von Karman constant is taken to be 0.4, the physical height above the ground z is known, and the displacement height d_o is taken to be 2/3 of the mean vegetation height if the field is covered by tall vegetation. Otherwise, d_o is set to 0 as explained in section 4.1.

The stability parameter ζ is defined as

$$\zeta \equiv \frac{-\kappa z g\left(\overline{w'\theta_v'}\right)_s}{\overline{\theta_v} u^{*3}}$$

where k, z and u^* are the von Karman constant, the height above the ground and the friction velocity as defined earlier in this section. The variable g is the acceleration of gravity, taken to be 9.81 m/s^2. The vertical heat flux $w'\theta_v'_s$ is measured by the eddy-correlation system. Finally, the mean virtual potential temperature is computed from the measured temperature, pressure and humidity.

Appendix 2: Values of ψ in the Roughness Sublayer I

In the unstable roughness sublayer, values of ϕ were observed to be smaller than the surface layer formulation (Garratt,1980 and Chen and Schwerdtfeger, 1989). How the smaller values of ϕ found in the roughness sublayer translate to values of ψ is investigated in this section. If the value ϕ in the roughness sublayer is β ($\beta < 1$) times the surface layer value ϕ throughout a certain stability range, then the value ϕ in the roughness sublayer becomes $\beta\phi$. The value β was found to be between 0.5 and 0.8 for $-10 < \zeta < 0$ in Garratt (1980). If $\beta\phi$ for the roughness sublayer is integrated to obtain the value ψ_{RS}, ψ_{RS} becomes

$$\psi_{RS} = \int_{\frac{z_{om}}{L}}^{\zeta} \frac{1-\beta\phi(\xi')}{\xi'} d\xi' \qquad \text{(A1)}$$

where the subscript RS indicates the roughness sublayer values. Equation (A1) can be rewritten as

$$\psi_{RS} = \int_{\frac{z_{om}}{L}}^{\zeta} \frac{1-\beta}{\xi'} d\xi + \beta \int_{\frac{z_{om}}{L}}^{\zeta} \frac{1-\phi(\xi')}{\xi'} d\xi' \qquad \text{(A2)}$$

thus,

$$\psi_{RS} = (1-\beta)\ln\left(\frac{z}{z_{om}}\right) + \beta\psi \tag{A3}$$

Whether ψ_{RS} for a given ζ becomes larger than ψ depends on whether $ln(z/z_{om})$ is larger than the value of ψ for a particular ζ. The value of ψ_{RS} is independent of the actual value of β. Thus, the smaller values of ϕ in the roughness sublayer reported in the literature imply neither larger nor smaller values of ψ.

Appendix 3: Values of ψ in the Roughness Sublayer II.

The mean wind profile in the surface layer can be expressed with equation

$$U = \frac{u*}{\kappa}\left[\ln\left(\frac{z}{z_{om}}\right) - \psi(\zeta)\right] \tag{4}$$

If we take the derivative of equation (4) with respect to z, it becomes

$$\frac{\partial U}{\partial z} = \frac{u*}{\kappa}\frac{\partial}{\partial z}\left[\ln\left(\frac{z}{z_{om}}\right) - \psi(\zeta)\right] \tag{A4}$$

$$\frac{\partial U}{\partial z} = \frac{u*}{\kappa}\left[\frac{1}{z} - \frac{\partial \psi(\zeta)}{\partial z}\right] \tag{A5}$$

If for a given flux the mean wind gradient in the roughness sublayer is smaller than in the surface layer at a given height, the gradient of $\psi(\zeta)$ in z in the roughness sublayer has to become larger than in the surface layer since $u*/\kappa z$ in (A5) is constant. Likewise, if the mean wind gradient in the roughness sublayer is larger than in the surface layer at a given height, the gradient of $\psi(\zeta)$ in z in the roughness sublayer has to become smaller than in the surface layer. In either case, a modification of the mean wind gradient in z influences the gradient of the values of ψ in z, but not necessarily the absolute values of ψ.

Appendix 4: Sensitivity Test of the Displacement Height

In the present study, the displacement heights (d_o) of BOREAS study sites are set to 2/3 of the average canopy height according to consensus although the methodologies of determining the displacement heights remain uncertain. Therefore, it is important to estimate the uncertainties of the momentum roughness length and values of ψ computed in the present study, associated with errors in the estimate of the displacement heights. The sensitivities of the momentum roughness length and values of ψ to changes in the displacement heights are tested with the BOREAS Old Aspen tower data from the 39.5m-level.

The average canopy height at the BOREAS OA site is 17.25 m, thus the displacement height is set to 11.5 m in the present study. For the sensitivity test, the displacement height is increased by 10 % and 20 % (d_o =12.7 m and d_o =13.8 m respectively). The momentum roughness lengths computed with the increased displacement heights are summarized in Table A1. The table indicates that the increased displacement height results in decreased momentum roughness length. However, a significant change (20%) in the displacement height results in a small decrease of the momentum roughness length (8.3% on average).

Figures A1 and A2 show the predicted and computed values of ψ plotted against the stability parameter ζ with d_o = 11.5m (reproduce of Figure 10a) and d_o = 13.8 m respectively. It is clear from the two figures that changing the displacement height by 20 % does not improve the fitting of the computed values

of ψ to the predicted values of ψ. The trend of the computed values of ψ is not altered noticeably by an increase of the displacement height by 20%.

In conclusion, uncertainties in the displacement height have little influence on the computed momentum roughness lengths and insignificant influence on the values of ψ reported in the present study.

Table A1. Momentum roughness lengths (m) of 8 wind directions with various displacement heights. In parentheses are the change in magnitude compared to the originals.

Wind	d_o = 11.5 m		d_o = 12.7 m (10%)		d_o = 13.8 m (20%)	
Directions	Daytime	Nighttime	Daytime	Nighttime	Daytime	Nighttime
0-45°	2.4	2.1	2.3 (-4.2%)	2 (-4.8%)	2.2 (-8.3%)	1.9 (-9.5%)
45-90°	2	2.1	1.9 (-5%)	2 (-4.8%)	1.8 (-10%)	1.9 (-9.5%)
90-135°	2.3	2.5	2.2 (-4.3%)	2.3 (-8.0%)	2.1 (-8.7%)	2.2 (-12%)
135-180°	1.7	1.8	1.6 (-5.9%)	1.7 (-5.6%)	1.6 (-5.9%)	1.6 (-11%)
180-225°	2.4	2.1	2.3 (-4.2%)	1.8 (-14%)	2.2 (-8.3%)	1.8 (-14%)
225-270°	2.6	2.6	2.5 (-3.8%)	2.5 (-3.8%)	2.4 (-7.7%)	2.4 (-7.7%)
270-315°	2	1.7	1.8 (-10%)	1.7 (0%)	1.8 (-10%)	1.6 (-5.9%)
315-360°	2.6	2.4	2.5 (-3.8%)	2.3 (-4.2%)	2.4 (-7.7%)	2.2 (-8.3%)
Average	2.3	2.2	2.1 (-5 %)	2.0 (-5.8%)	2.1 (-8.3%)	2.0 (-9.8%)

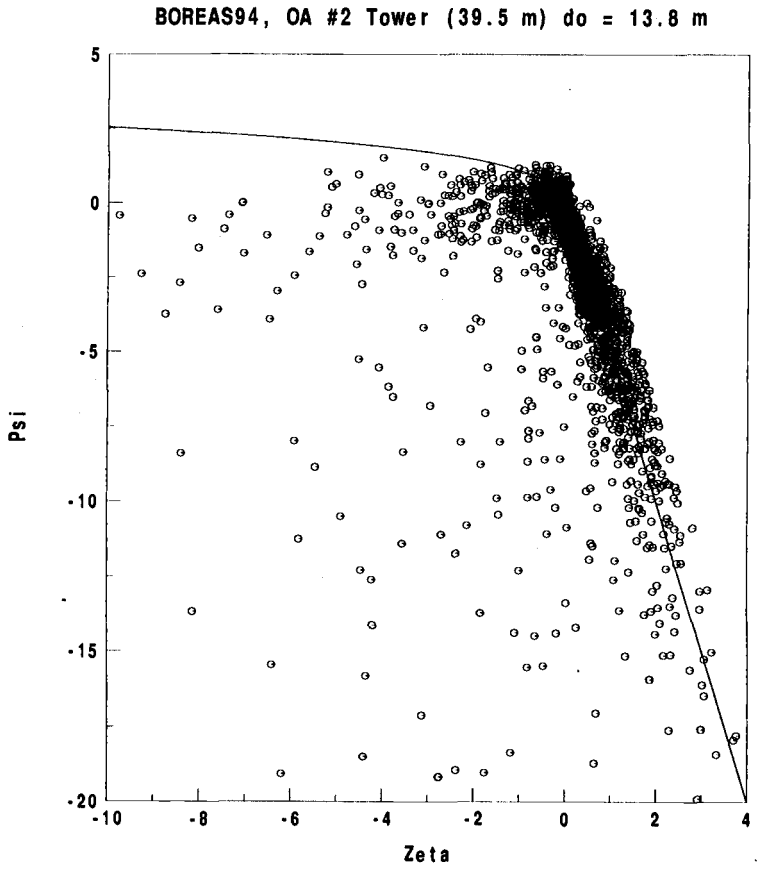

A1

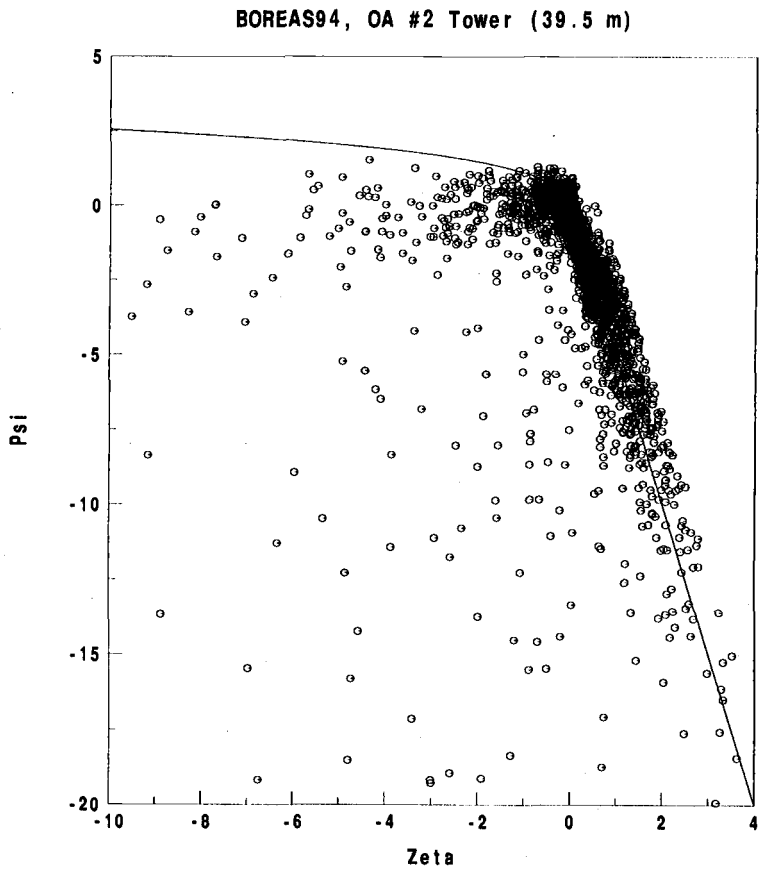

A2

Figure A1. Computed and predicted values of ψ (dots and line, respectively) plotted against the stability parameter ζ for all wind directions at the BOREAS Old Aspen site. The displacement height is 13.8 m.

Figure A2. Same as Figure A1 except 11.5 m for the displacement height (reproduce of Figure 10a).

Appendix 5: Random Flux Sampling Errors and Values of ψI

Flux measurements are always subject to random flux sampling errors (RFE). The BOREAS tower flux measurements, on which the computations of momentum roughness lengths and values of ψ in the present study are based, are not an exception. In Section 5.2, the computed values of ψ for the BOREAS tower flux measurement heights are found to be systematically smaller than the predicted values of ψ in unstable conditions (Paulson, 1970). Without a flux sampling error analysis, the suspicion that this result is associated with sampling flux errors remains.

In order to illustrate that the result is independent of random flux sampling errors, the BOREAS Old Aspen tower data set III from the 39m-level is examined since the random flux errors are computed for this data set. The random flux sampling error is defined in Vickers and Mahrt (1997). The BOREAS OA tower data set data set III is based on the same BOREAS OA tower raw data as the BOREAS OA TF tower data analyzed in the other sections of the present study. However, the fluxes and other variables are computed differently between the two data sets. The main differences between the two data sets are compared in Table A2.

Table A2. Comparison of BOREAS Old Aspen TF tower data set and BOREAS Old Aspen tower data set III

		BOREAS Old Aspen TF Tower Data Set	BOREAS Old Aspen Tower Data Set III
Fluxes	Flux filtering window	30 minutes	10 minutes
	Flux averaging window	30 minutes	1 hour
Wind Speed	Averaging methods	Scalar average	Vector average
	Time for averaging wind speed	30 minutes	1 hour
Time for averaging other variables		30 minutes	1 hour

The procedure in Sections 4.1 and 5.2 are followed to compute the momentum roughness length and values of ψ with the BOREAS OA tower data set III except for a single modification. Since the wind direction is not available in the BOREAS OA tower data set III, the dependency of the momentum roughness length on the wind speed direction is not examined. The momentum roughness lengths computed with the current analysis are shown in Table A3 and the computed and predicted values of ψ are plotted in Figure A3. Figure A3 shows that the trend of the computed values of ψ remains very similar to that found in Figure 10a despite different processing of the raw data between the two data sets.

Now, the data for which the momentum and heat fluxes have random flux sampling errors of less than ± 0.5 are analyzed. Applying this criterion of the random flux sampling errors eliminates 11.8% and 8.8% of the original data points for the daytime and nighttime respectively. The results of the analysis are found in

Table A3 and Figure A4. Figure A4 clearly indicates that the computed values of ψ being smaller than the predicted values of ψ in unstable conditions for OA site are not associated with the random flux sampling errors.

Table A3. Comparison of momentum roughness lengths (m) computed with BOREAS OA tower data. The momentum roughness lengths reported for BOREAS OA TF Tower data are the average values of the 8 wind directions. (RFE stands for random flux error)

	BOREAS OA TF Tower Data	BOREAS OA Tower Data III All RFE	BOREAS OA Tower Data III, $\|RFE\| < 0.5$
Daytime	2.2	2.1	2.0
Nighttime	2.2	2.0	2.0

All RFE

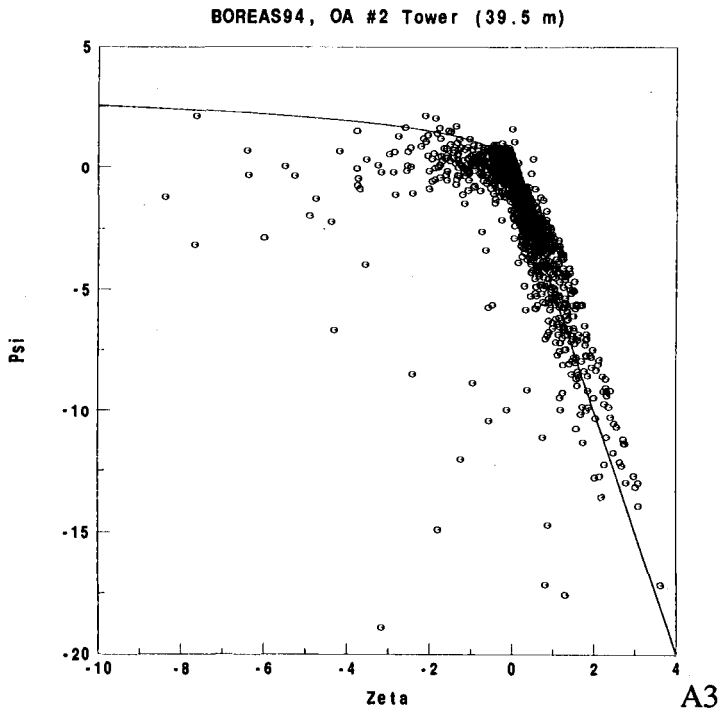

A3

|RFE| < 0.5

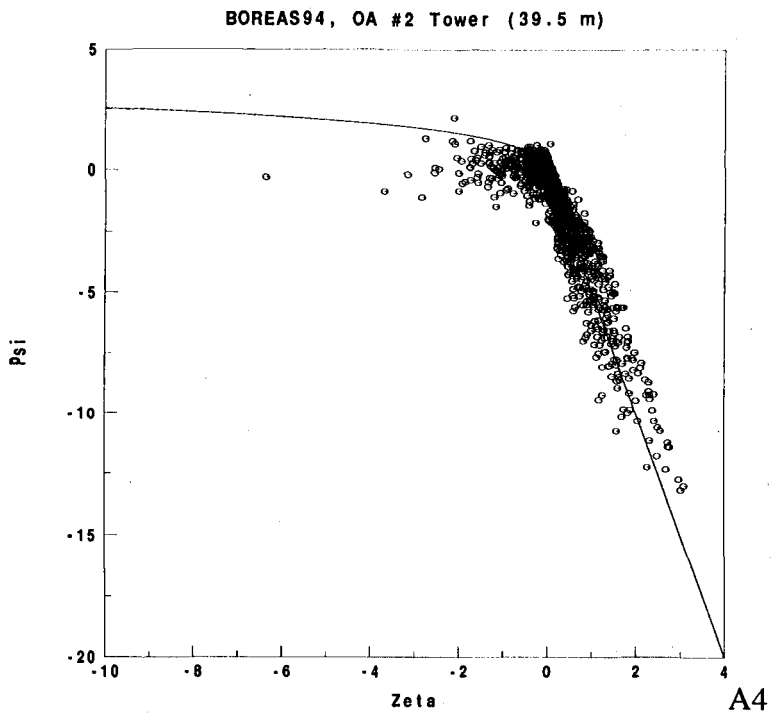

A4

Figure A3. Computed and predicted values of ψ (dots and line, respectively) plotted against the stability parameter ζ for all wind directions at the BOREAS Old Aspen site. The results are based on BOREAS OA tower Data III.

Figure A4. Same as Figure A3 except for |RFE| < 0.5.

Appendix 6: Random Flux Sampling Errors and Values of ψ II

This section examines how the random flux sampling errors may propagate to the computed values of ψ with the BOREAS OA tower data set III. For this purpose, the maximum and minimum possible one-hour-averaged momentum and heat fluxes are computed based on the random flux sampling errors. To simplify the study, it is assumed that the maximum possible heat flux is accompanied by the maximum possible momentum flux and vice versa. Furthermore, only the daytime and nighttime data, for which the momentum and heat fluxes have random flux sampling errors of less than ±0.5, are analyzed to avoid unreliable flux data.

Table A4 lists the momentum roughness lengths computed with the maximum and minimum possible momentum and heat fluxes. The momentum roughness lengths change noticeably with reduced fluxes. Figures A5 and A6 show the values of ψ computed with original, maximum and minimum flux values for fluxes with $|RFE| < 0.5$. In highly stable conditions, with modified fluxes, the scatter of computed ψ as well as the deviation of computed ψ from the predicted values become larger than with the original fluxes (Figure A4). In unstable conditions, the computed values of ψ remain smaller than the predicted values both with the maximum and minimum possible fluxes. These results confirms that uncertainties associated with random flux sampling errors do not explain the smaller values of computed ψ in comparison to the predicted ψ from Paulson (1970) in unstable conditions.

Table A4. Comparison of momentum roughness lengths (m) computed with BOREAS OA tower data set III. (RFE, mfx and hfx stand for random flux error, momentum flux and heat flux respectively.)

	All RFE	|RFE| < 0.5	|RFE| < 0.5, max mfx, hfx	RFE| < 0.5, min mfx, hfx
Daytime	2.1	2.0	2.3	1.7
Nighttime	2.0	2.0	2.1	1.6

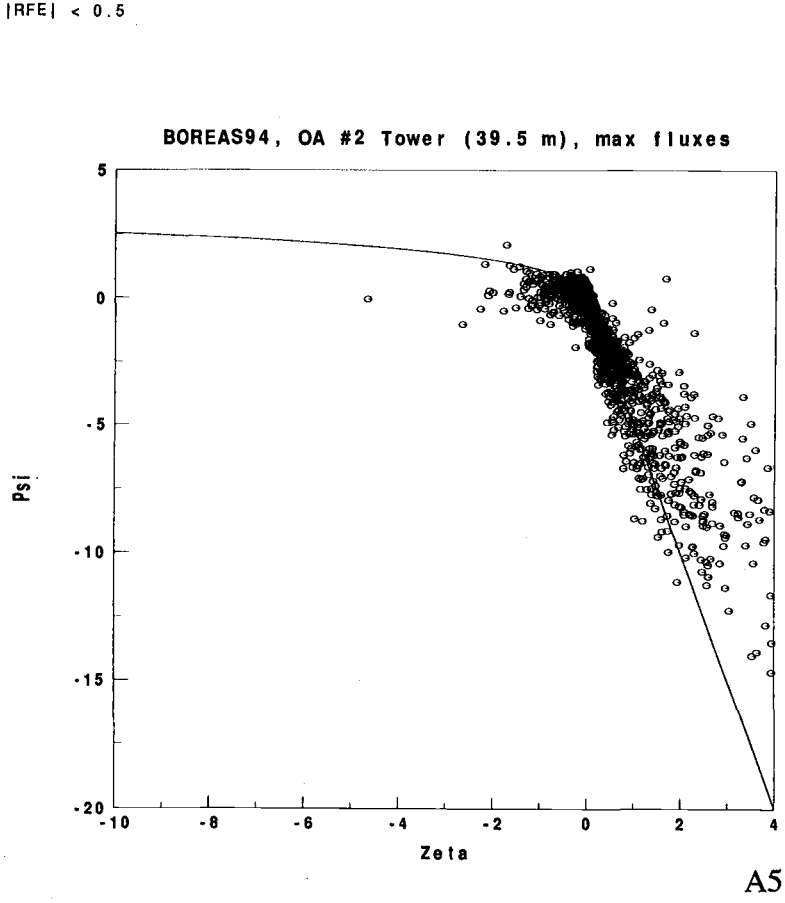

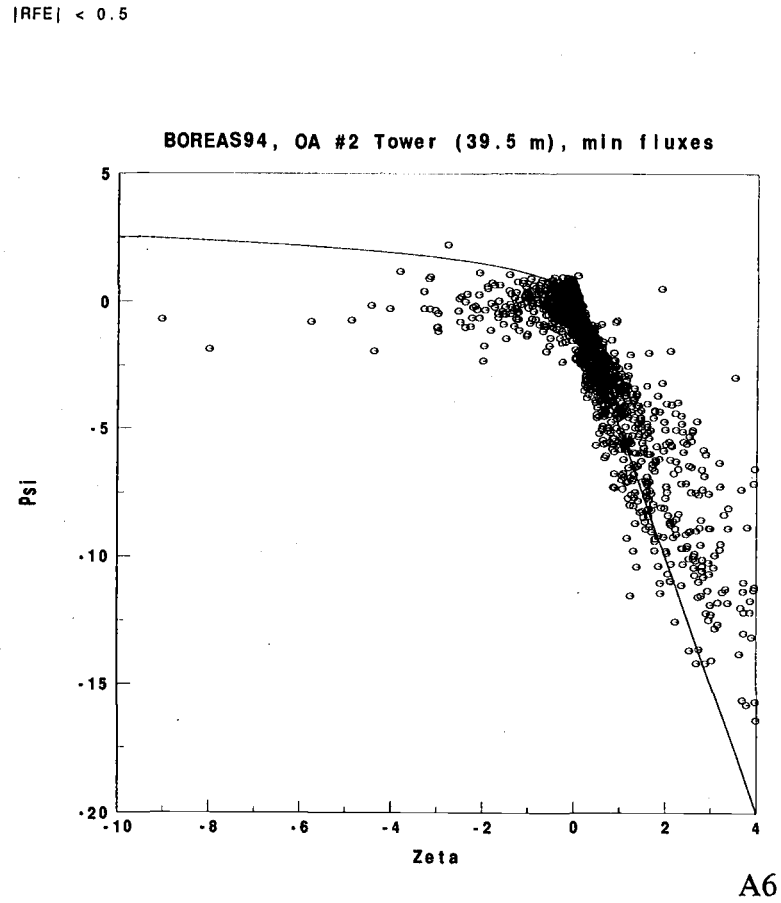

Figure A5. Computed and predicted values of ψ (dots and line, respectively) plotted against the stability parameter ζ for all wind directions and for |RFE| < 0.5 at the BOREAS Old Aspen site. The results are based on maximum possible fluxes according to random flux errors.

Figure A6. Same as Figure A5 except for minimum possible fluxes according to random flux errors.